Giant Resonances

Fundamental Collective Modes of Nuclear Excitation

Charge-Exchange Modes

Muhsin N. Harakeh

University of Groningen, the Netherlands

3rd NUclear physics School for Young Scientists (NUSYS)

Fudan University, Shanghai

6-12 August 2023

university of groningen

Giant Resonances in hydrodynamic models

Coherent vibrations of nucleonic fluids (p & n; ↑ & ↓) in a nucleus

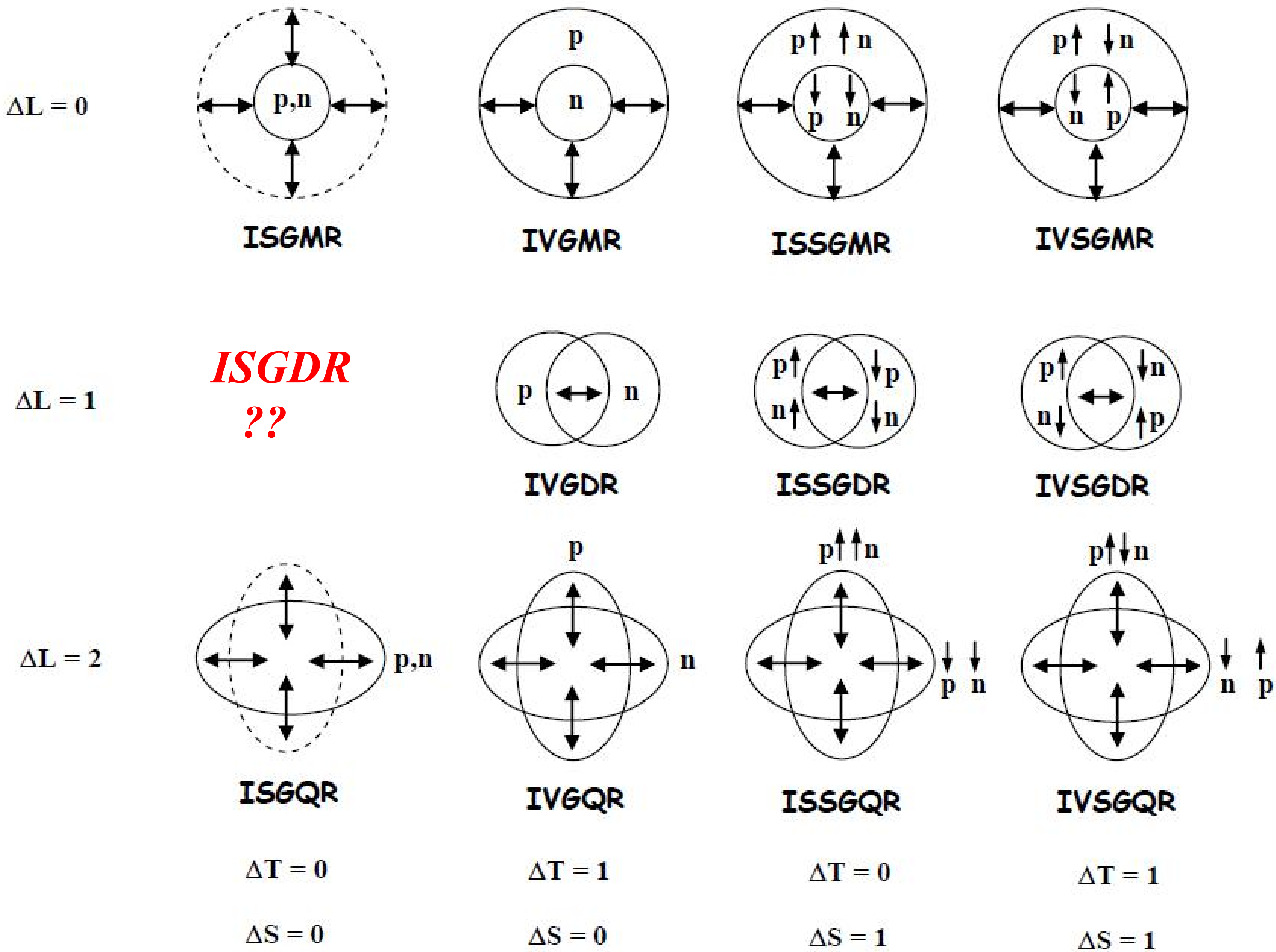

Spin-isospin excitations

Neutral (ν,ν') and charged (ν_e,e^-), ($\bar{\nu}_e,e^+$) currents

NC $\Rightarrow$ Inelastic electron and proton scattering

$\Rightarrow$ *M0*, *M1*, *M2*

CC $\Rightarrow$ Charge-exchange reactions

Isovector charge-exchange modes

$\Rightarrow$ IAS, GTR, IVSGMR, IVSGDR, etc.

Importance for nuclear astrophysics,

ν-physics, 2β-decay, *n*-skin thickness, etc.

(p,n), (^{3}He,t) {GT^-}; (n,p), (d,^{2}He) & (t,^{3}He) {GT^+}

Nucleus → **Many-body system with a finite size**

Vibrations → **Multipole expansion with r, Y_{lm}, τ, σ**

	$\Delta S=0, \Delta T=0$	$\Delta S=0, \Delta T=1$	$\Delta S=0, \Delta T=1$	$\Delta S=1, \Delta T=1$	$\Delta S=1, \Delta T=1$
$L=0$: Monopole	**ISGMR** $r^2 Y_0$	**IAS** τY_0	**IVGMR** $\tau r^2 Y_0$	**GTR** $\tau \sigma Y_0$	**IVSGMR** $\tau \sigma r^2 Y_0$
$L=1$: Dipole	**ISGDR** $(r^3 - 5/3\langle r^2 \rangle r) Y_1$		**IVGDR** $\tau r Y_1$		**IVSGDR** $\tau \sigma r Y_1$
$L=2$: Quadrupole	**ISGQR** $r^2 Y_2$		**IVGQR** $\tau r^2 Y_2$		**IVSGQR** $\tau \sigma r^2 Y_2$
$L=3$: Octupole	**LEOR, HEOR** $r^3 Y_3$				

Dropped $\Delta S=1, \Delta T=0$ operators because excitations are very weak

Non-Energy-Weighted Sum Rules

Fermi, Gamow-Teller and higher multipole non-energy-weighted sum rules (NEWSR):

$$\beta_{\pm}(\mu) = \frac{1}{2}\sum_{k=1}^{A} \sigma_{\mu k}\tau_{\pm k} \Rightarrow S_{\pm}(GT) = \sum_{f,\mu} |\langle f|\beta_{\pm}(\mu)|i\rangle|^{2}$$

$$S_{-}(GT) - S_{+}(GT) = 3(N - Z)$$

This is the Ikeda sum rule for GT transitions.

For the Fermi sum rule (IAS):

$$S_{\pm}(F) = \frac{1}{4}\sum_{f,\mu} |\langle f|\tau_{\pm}|i\rangle|^{2} \Rightarrow S_{-}(F) - S_{+}(F) = (N - Z)$$

For isovector non-spin-flip and isovector spin-flip higher multipole operators:

$$S_{-}^{\lambda J} - S_{+}^{\lambda J}(J) = \frac{3(2J+1)}{2\pi}\left(N\langle r_n^{2\lambda}\rangle - Z\langle r_p^{2\lambda}\rangle\right)$$

If spin-flip is involved the sum over possible *J*-values yields a factor 3(2λ+1).

Gamow-Teller excitations and Astrophysical Implications

Spin-isospin excitations

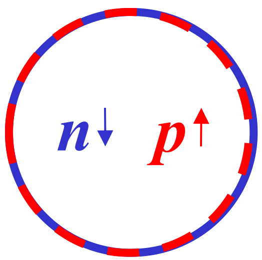

$\Delta L = 0$ $\Delta S = 1$ $\Delta T = 1$

GTR

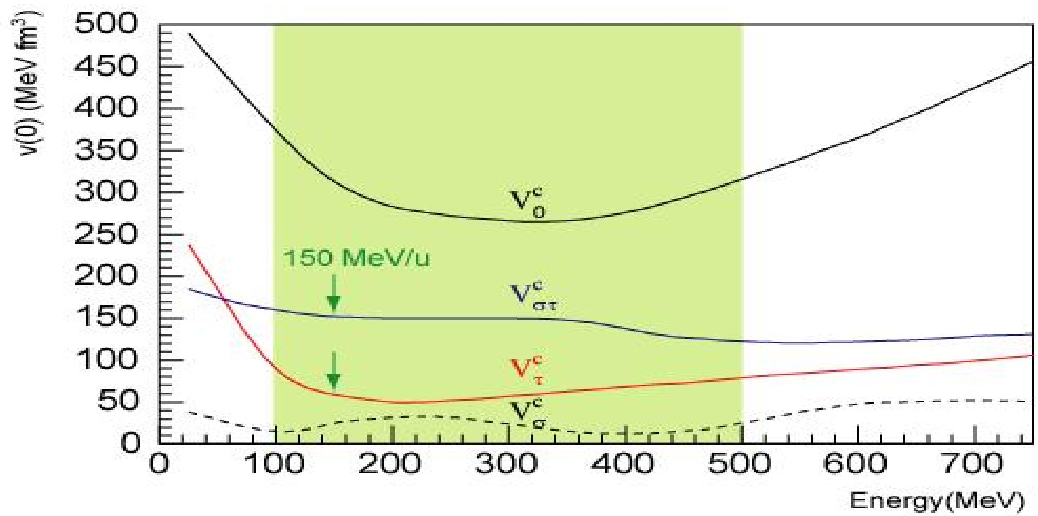

- **Gamow-Teller transitions;**

  Isospin ($\Delta T = 1$)

  Spin ($\Delta S = 1$)

Advantages

- **Cross section peaks at $\theta = 0°$ ($\Delta L = 0$)**
- **Strong excitation of GT states at E = 100-500 MeV/u**

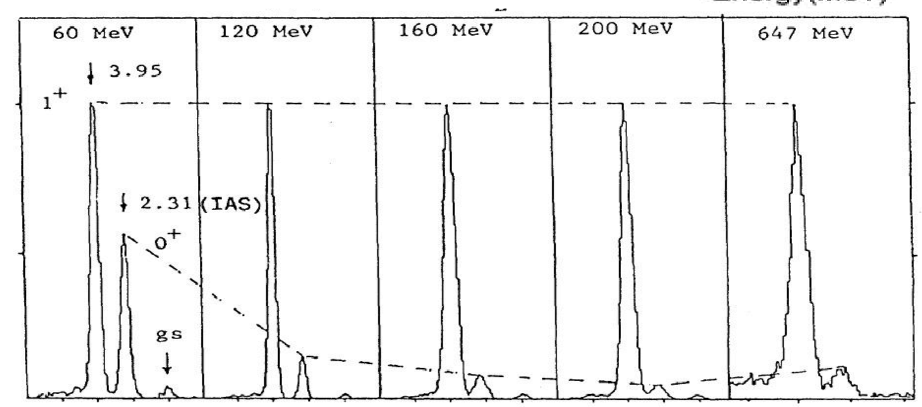

FIG. 4. Zero-degree cross-section spectra for the $^{14}C(p,n)^{14}N$ reactions at the indicated bombarding energies. The spectra have been arbitrarily normalized. From Gaarde (1985) and Rapaport (1989).

J. Rapaport, E. Sugarbaker, Annu. Rev. Nucl. Part. Sci. 44 (1994) 109

Spin-flip & GT transitions

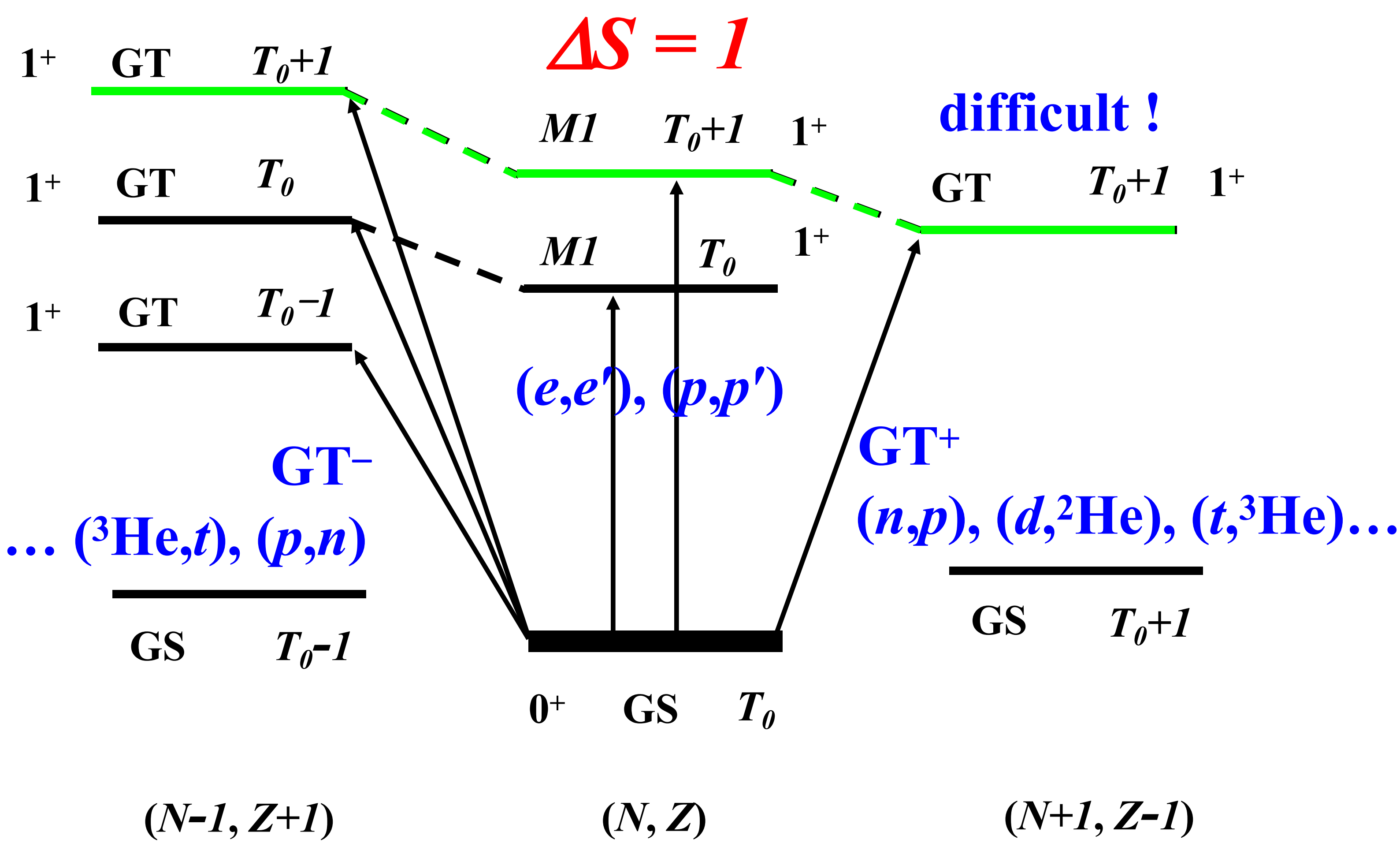

Charge-exchange probes

(*p*,*n*)-type ($\Delta T_z = -1$)

- β^--decay
- (*p*,*n*)
- (^{3}He,*t*)
- heavy ion

(*n*,*p*)-type ($\Delta T_z = +1$)

- β^+-decay
- (*n*,*p*)
- (*d*,^{2}He)
- (*t*,^{3}He)
- heavy ion; (^{7}Li,^{7}Be)

- Energy per nucleon (>100 MeV/u)
- Spin-flip versus non-spin-flip
- Complexity of reaction mechanism
- Experimental considerations

The (*p*,*n*) reaction at 0 degree

- **Cross sections at $E_p \geq 100$ MeV, $q = 0$ for (*p*,*n*) reactions**

$$\frac{d\sigma}{d\Omega} = \frac{\mu_i \mu_f}{(\pi\hbar^2)^2}\left(\frac{k_f}{k_i}\right)(N_\tau^D |J_\tau|^2 B(F) + N_{\sigma\tau}^D |J_{\sigma\tau}|^2 B(GT))$$

N^D= σ(DW; 0)/σ(PW; 0) is distortion factor.

J represents the volume integral of the relevant NN interaction component.

T. N. Taddeucci *et al*., Nucl. Phys. A469 (1987) 125

I. Bergqvist *et al*., Nucl. Phys. A469 (1987) 648

- **Neutrino absorption cross sections**

$$\sigma = \frac{1}{\pi \hbar^4 c^3}\left[G_V^2 B(F)^2 + G_A^2 B(GT)^2\right] \times F(Z, E_e) p_e E_e$$

***F*(*Z*,*E*$_e$) is the relativistic Coulomb barrier factor**

Importance of charge-exchange reactions at intermediate energies

Time of flight (ToF) neutron spectra for $^{90}Zr(p, n)^{90}Nb$ reaction at E_p= 120 MeV

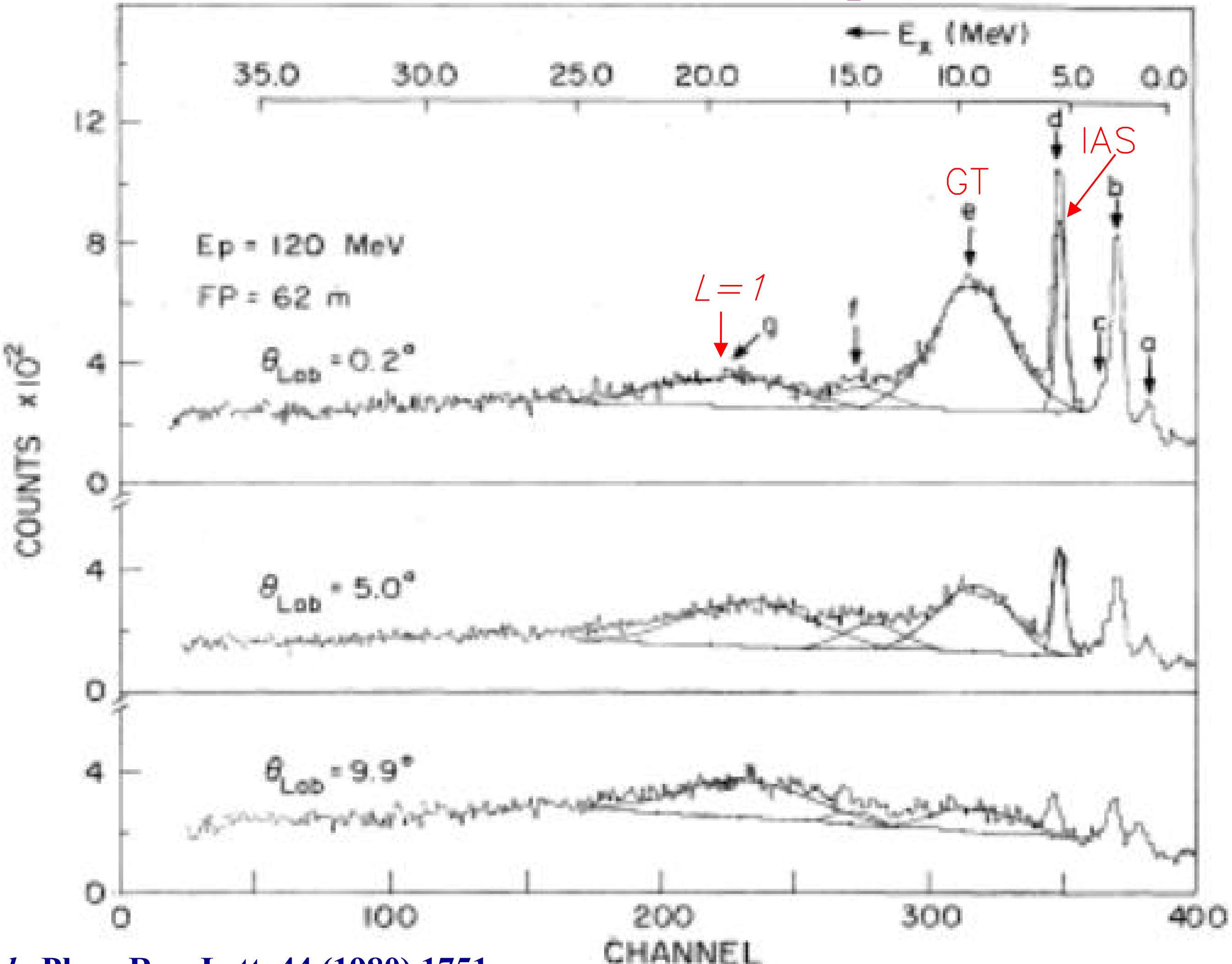

D.E. Bainum *et al.*, Phys. Rev. Lett. 44 (1980) 1751

(p, n) excitation-energy spectra for Fe and Ni Isotopes from ToF measurements

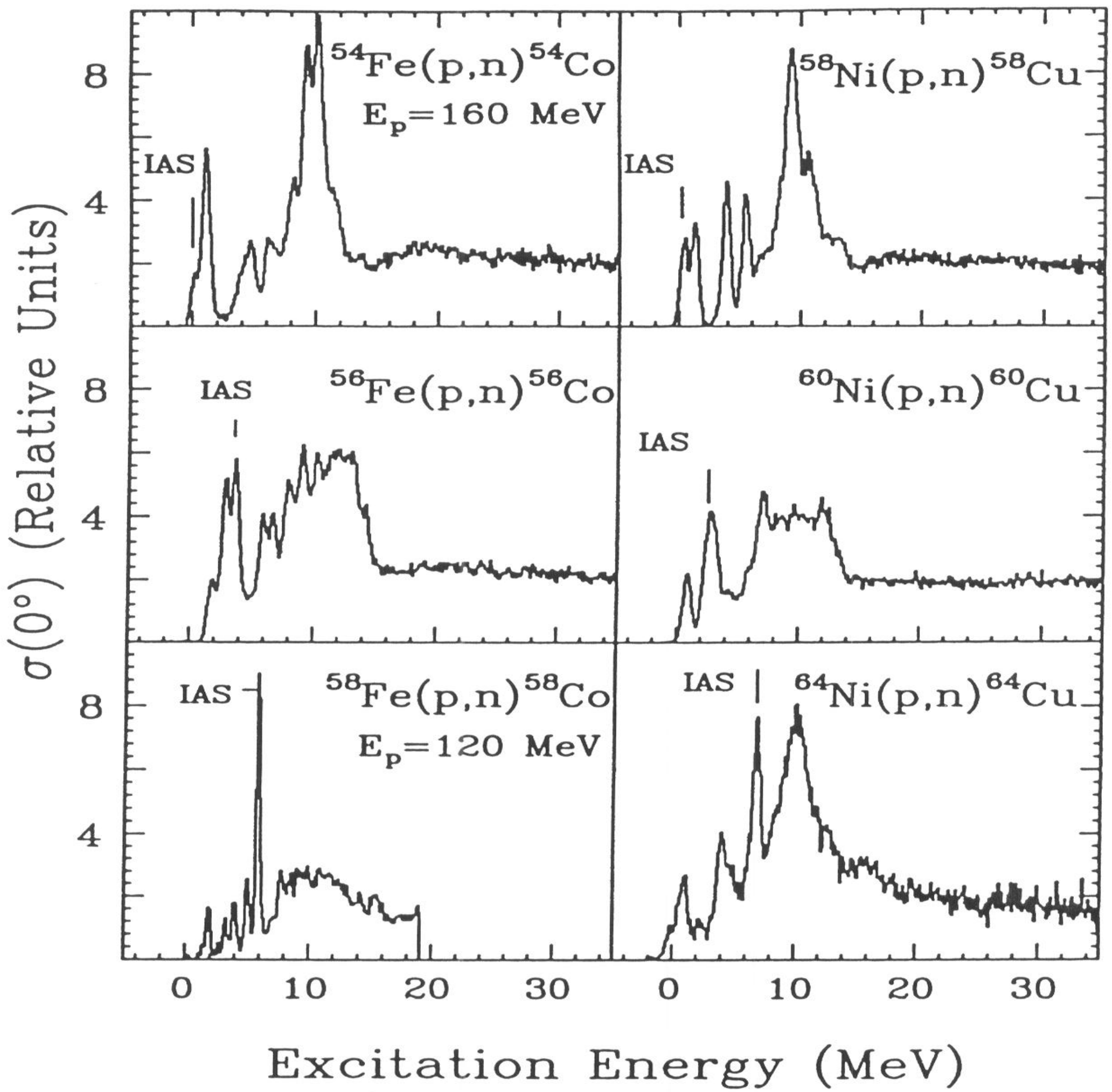

Zero-degree (p,n) spectra for even Fe and even Ni isotopes at E_p = 160 MeV.

The ^{58}Fe(p,n)^{58}Co spectrum was obtained at E_p = 120 MeV.
⇒ Relatively stronger excitation of IAS

J. Rapaport, E. Sugarbaker, Annu. Rev. Nucl. Part. Sci. 44 (1994) 109

situation before 1997

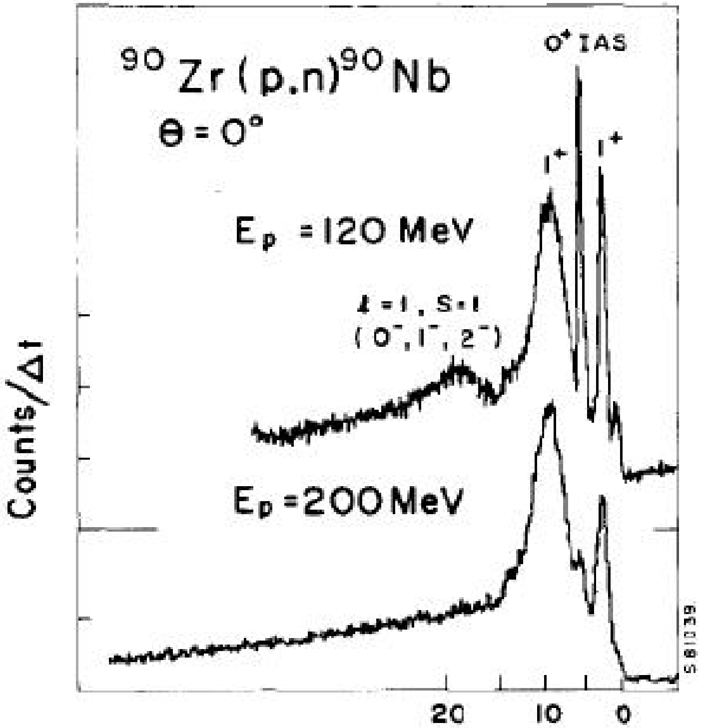

The quenching problem of GT strength

1- Pushed to higher energies by tensor force, A. Arima *et al.;* or

2- Coupling to Δ resonance, M. Ericson *et al.*

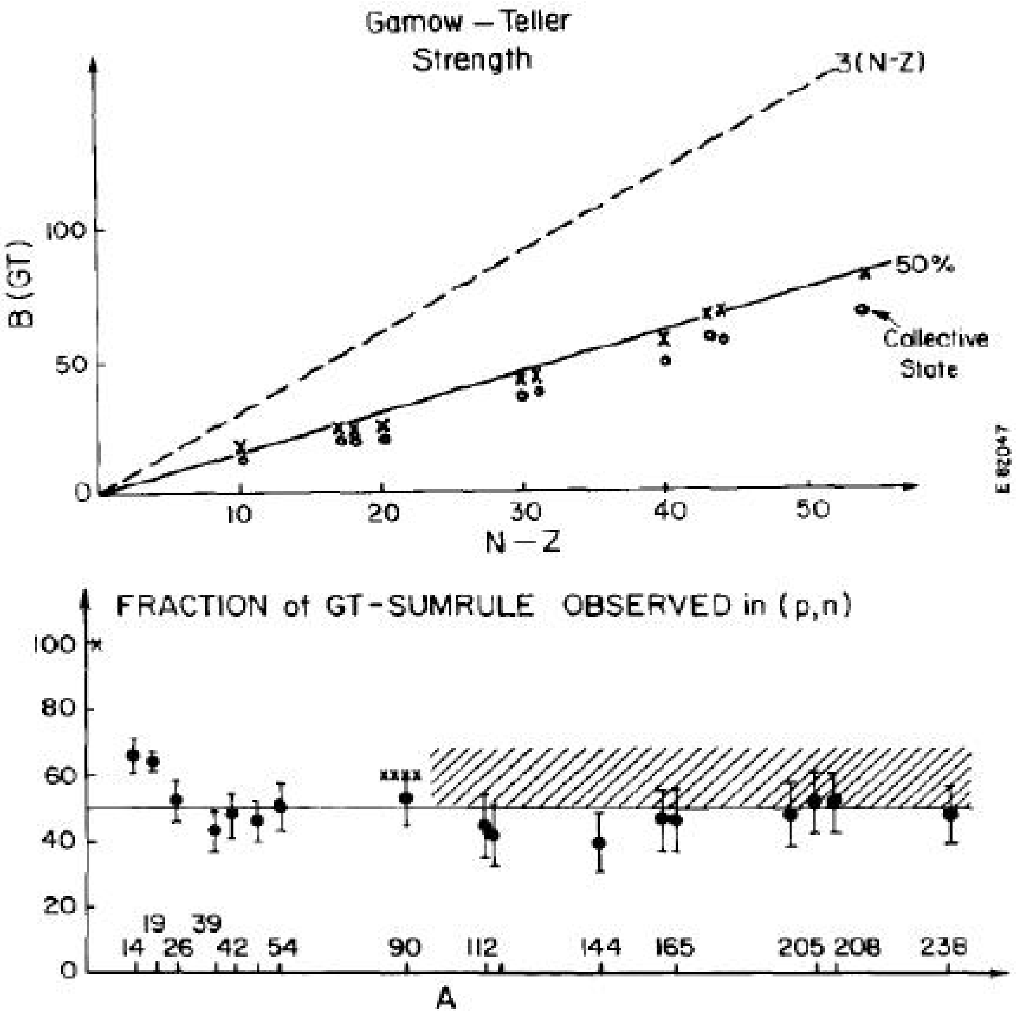

C. Gaarde, Nucl. Phys. A396 (1983) 127c

university of groningen

$^{90}Zr\ (p,n)\ ^{90}Nb$

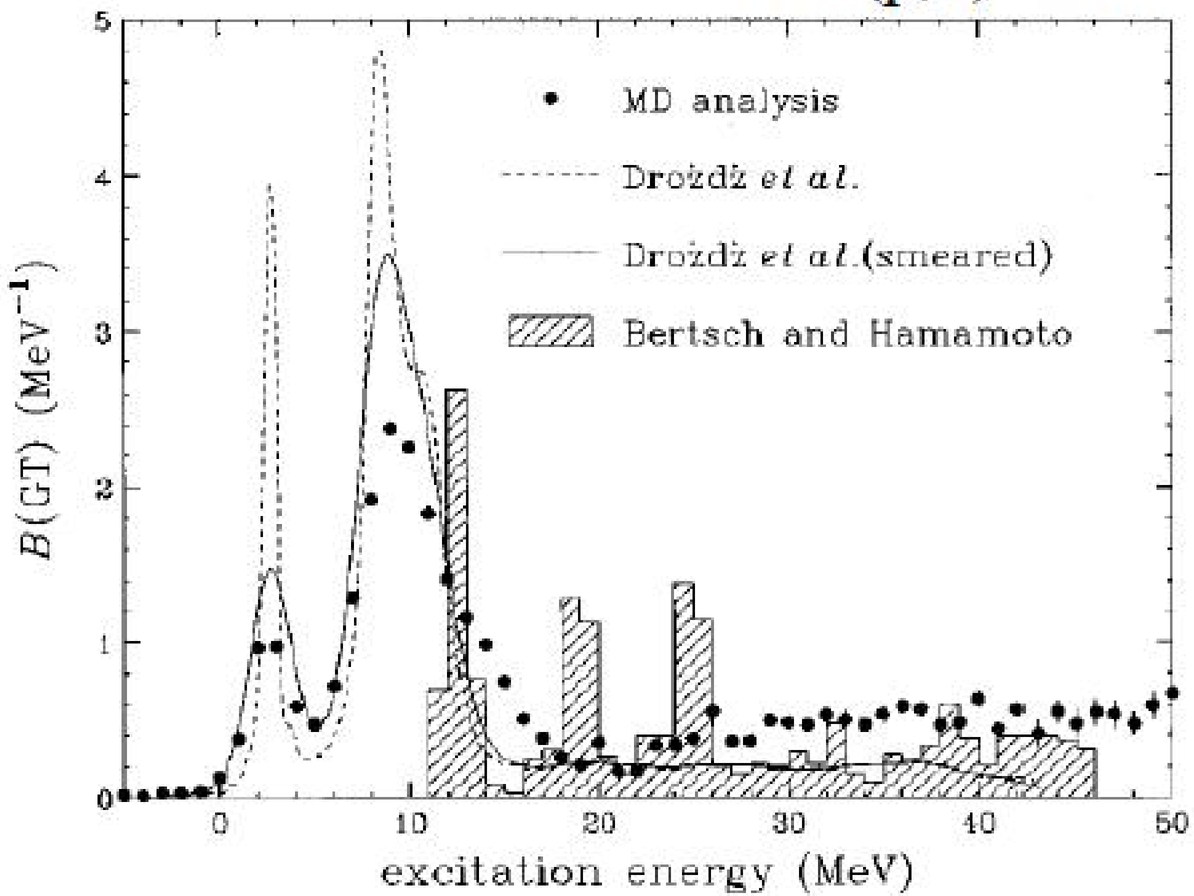

T. Wakasa et al., PRC55 ('97) 2909

$S_- - S_+ = 27.0 \pm 1.6 = (90 \pm 5)\%$ of Ikeda sum rule

⇒ *Δ* contribution is small **T. Wakasa *et al.*, Phys. Rev. C 55 (1997) 2909**

university of groningen

(^{3}He,t) Reaction ≥ 100 MeV/u

- **Energy dependence of effective interactions.**

- **At RCNP, Osaka**

  $E(^3\text{He}) \approx 150$ MeV/u

  - **V_0 part: Near Minimum.**
  - **$V_{\sigma t}$ part: Relatively large.**
  - **V_t part: Minimum.**
  - **V_σ part: Negligible**

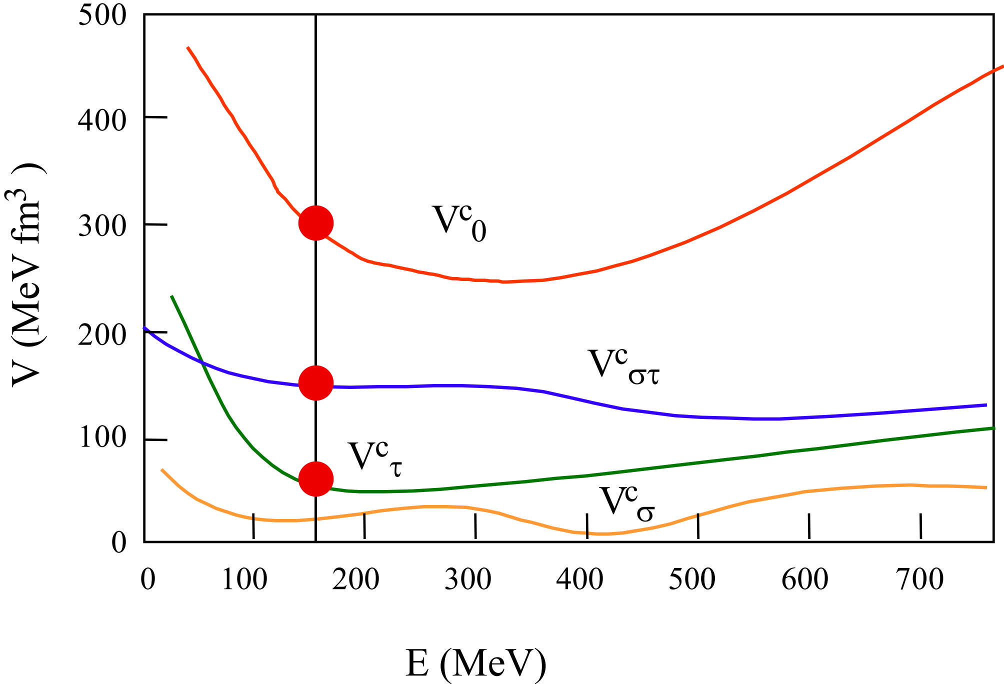

The (^{3}He,*t*) reaction at 0 degree
Measuring GT strengths

Cross sections at $E(^3\text{He}) = 450$ MeV, $q = 0$ for (^{3}He,*t*) reactions

$$\frac{d\sigma}{d\Omega}(q=0) = KN_D\left|J_{\sigma\tau}\right|^2 B(GT)$$

kinematic factor

distortion factor

nucleon-nucleus interaction

Gamow-Teller strength

Calibration of *B(GT)* to cross sections for known transitions (e.g., from β-decay)

Experiments at RCNP, Osaka University

- (^{3}He,*t*) reaction at 420 MeV
  - High-resolution spectrometer “Grand Raiden”
  - $\Delta E \sim 30$ keV

Beam line WS-course

Grand-Raiden Spectrometer

M. Fujiwara *et al.*, NIM A422 (1999) 484

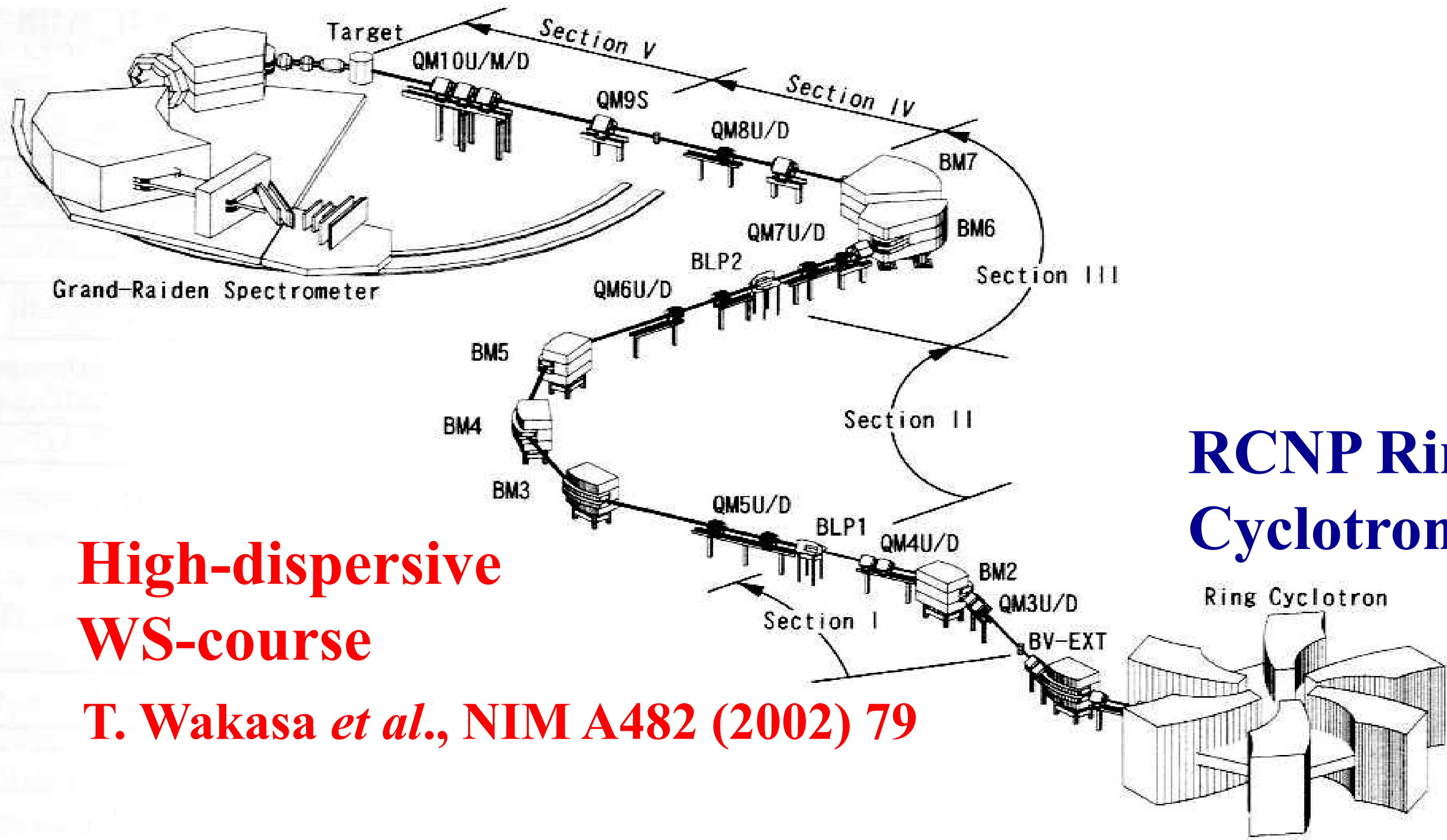

RCNP Ring Cyclotron

High-dispersive WS-course

T. Wakasa *et al.*, NIM A482 (2002) 79

Used ^{164}Dy(^{3}He,*t*)^{164}Ho (g.s., 1$^+$) reaction for calibration: log*ft* 4.6 → *B(GT)* = 0.293±0.006

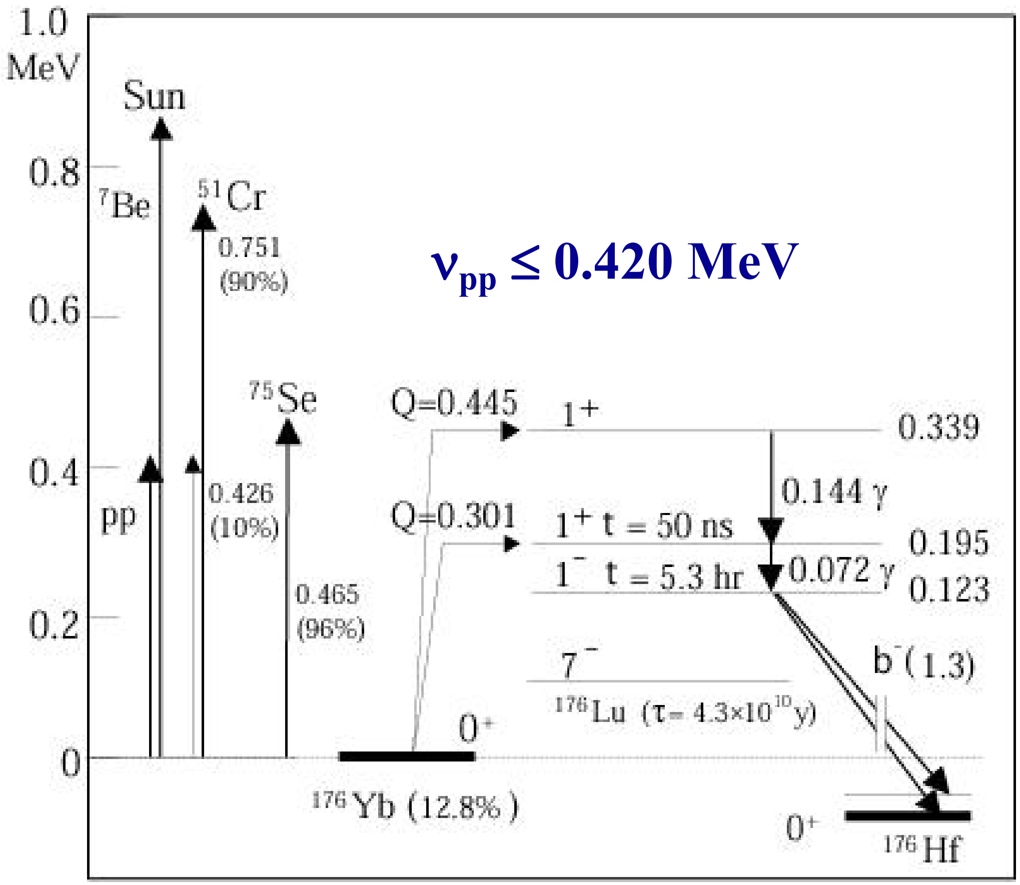

M. Fujiwara *et al.*, PRL 85 (2000) 4442

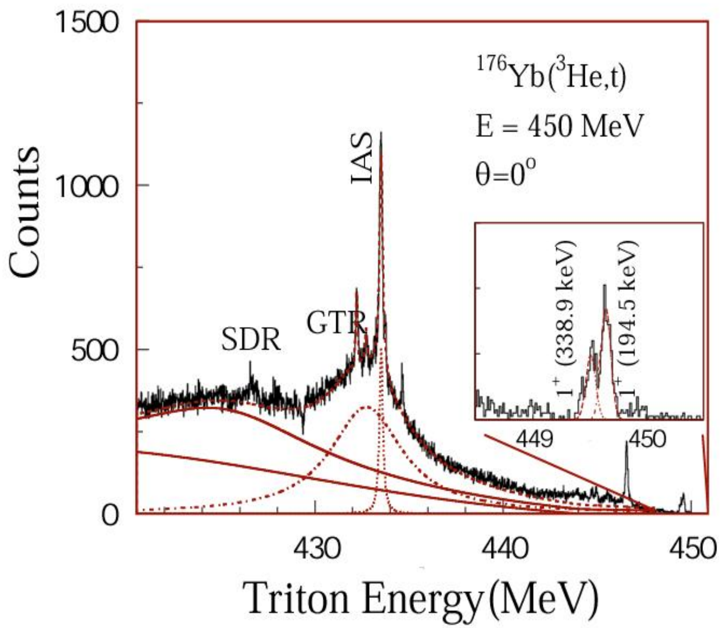

Resolution ≈ 100 to 130 keV

E_x(MeV)	0.195+0.339 (*p,n*)	0.195 (^{3}He,*t*)	0.339 (^{3}He,*t*)
B(GT)	0.32±0.04	0.20±0.04	0.11±0.02

Evolution of Resolution in Charge-Exchange Reactions at Intermediate Energies

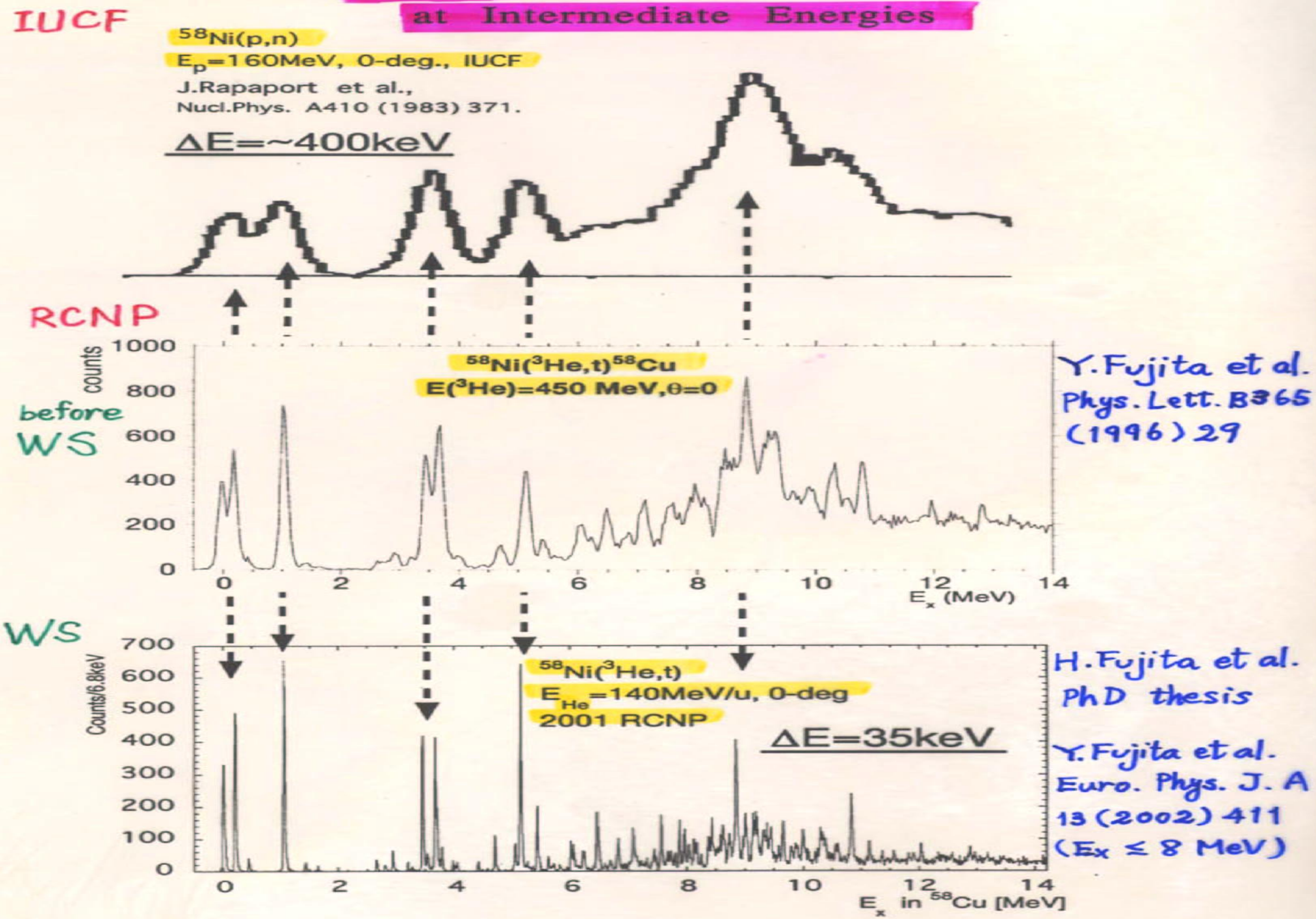

university of groningen

Decomposition of the isospin components of the excited states in ^{58}Cu.

- Isospin of ^{58}Ni g.s. : $T_0 = 1$

- In principle, comparison among (n,p), (p,p'), (p,n) spectra

  → separates isospin components

But, very difficult in practice because of high level density for $T = 1$ and $T = 2$ states.

- Clebsch-Gordon coefficients for ($T_0 = 1$)

$\Rightarrow$ $\sigma_{T=0}:\sigma_{T=1}:\sigma_{T=2}$ = 2:3:1 for (p,n)

$\Rightarrow$ $\sigma_{T=1}:\sigma_{T=2}$ = 1:1 for (p,p'), (e,e')

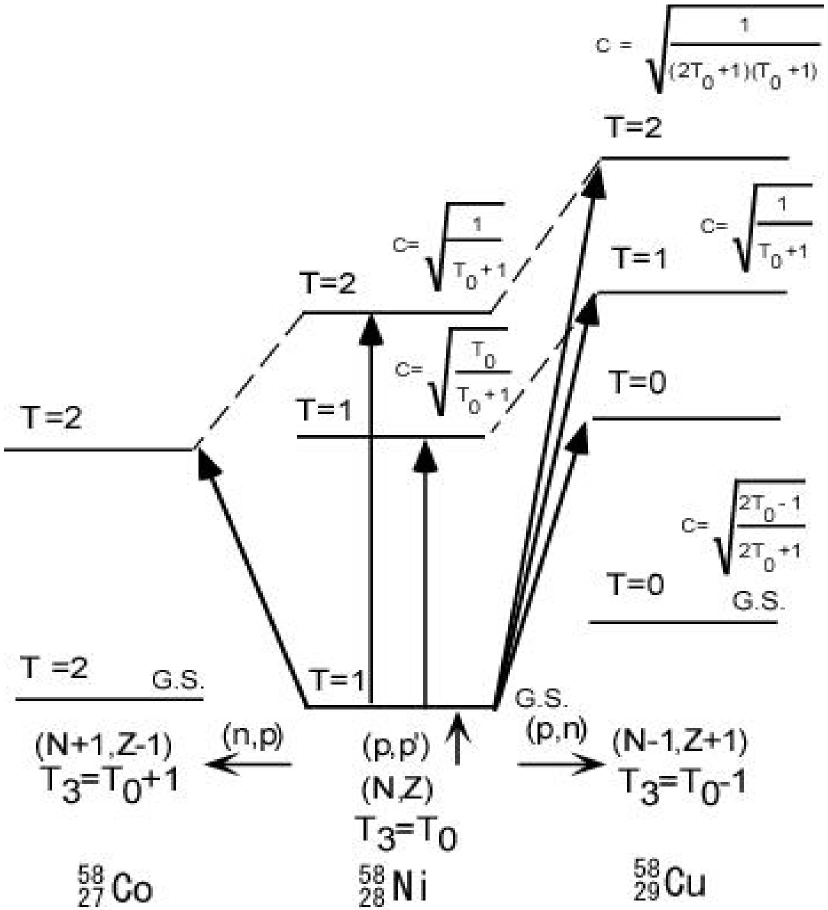

university of groningen

Comparison of (^{3}He,*t*) and (*e*,*e′*) spectra

- Comparison of 1^+ levels in (^{3}He,*t*) with (*e*,*e′*) and (*t*,^{3}He) spectra
  - ➔ Try to separate isospin components
- Fig. (b) is shifted by 0.20 MeV (IAS)
  - b-1) B(M1) distribution obtained in (*e*,*e′*)
  - b-2) B(M1) convoluted with 140 keV resolution, to match (^{3}He,*t*) spectra
  - In b-1) 1^+ levels observed in (*t*,^{3}He) spectra are marked with small circles Furthermore, comparing with (*n*,*p*) spectra assume all levels above 11.5 MeV have *T*=2
  - b-3) Same as b-2) but with *T*=2 strength reduced artificially by a factor 3
- At $E_x \sim$ 6-10 MeV (*T=1* region)
  - Rather good correspondence
- At $E_x \sim$ 10-15 MeV (*T=2* region)
  - Reasonable correspondence

Y. Fujita *et al.*, Phys. Lett. B365 (1996) 29

Y. Fujita *et al.*, Eur. Phys. J. A13 (2002) 411

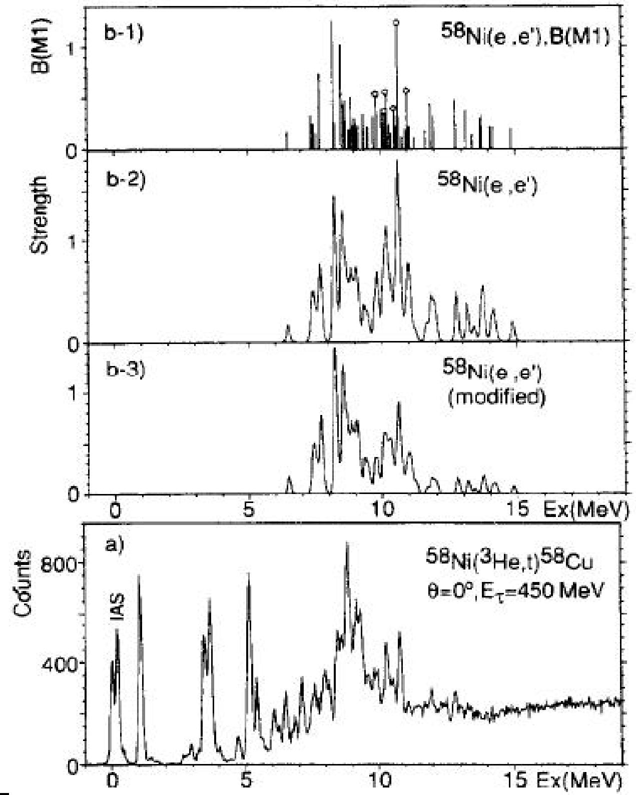

B(M1) distribution

Γ_{FWHM} = 30 keV

σ(T=1):σ(T=2)

= 1 : 1

σ(T=2)/3

σ(T=1):σ(T=2)
= 3 : 1

Γ_{FWHM} = 140 keV

Before WS beam line

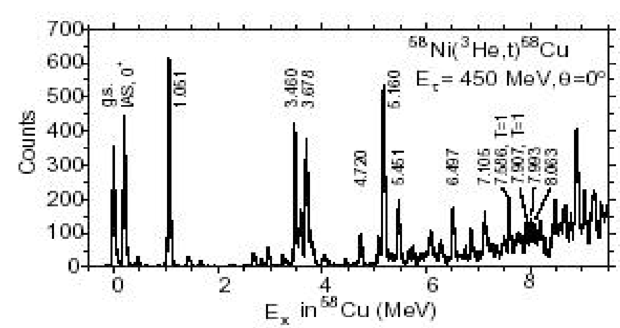

WS beam line

Γ_{FWHM} = 50 keV

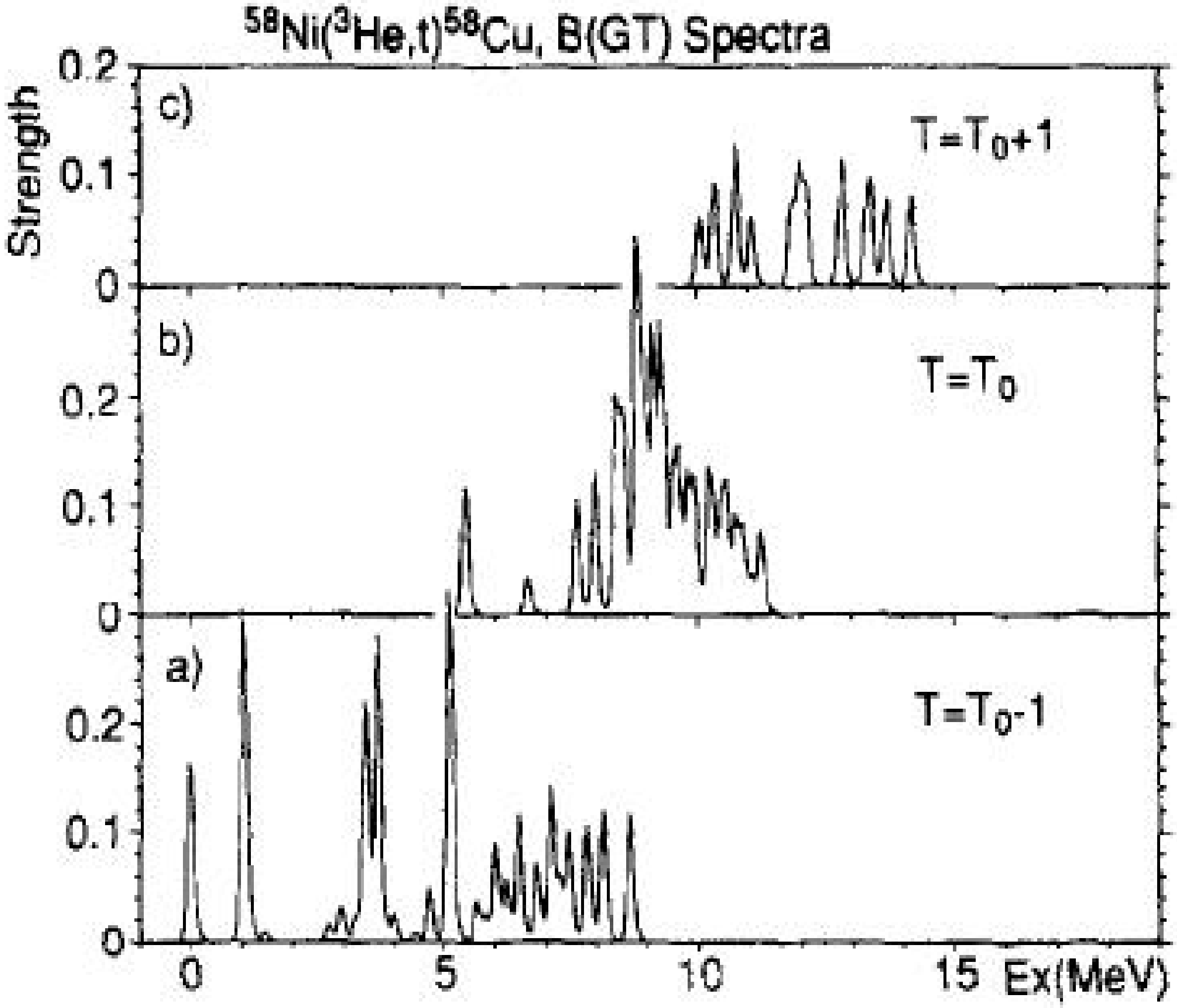

Disentangling the isospin components of the GT strength in ^{58}Cu

See: Y. Fujita *et al.*, Phys. Lett. B365 (1996) 29

^{54}Fe(p,n) & ^{54}Fe(^{3}He,t)

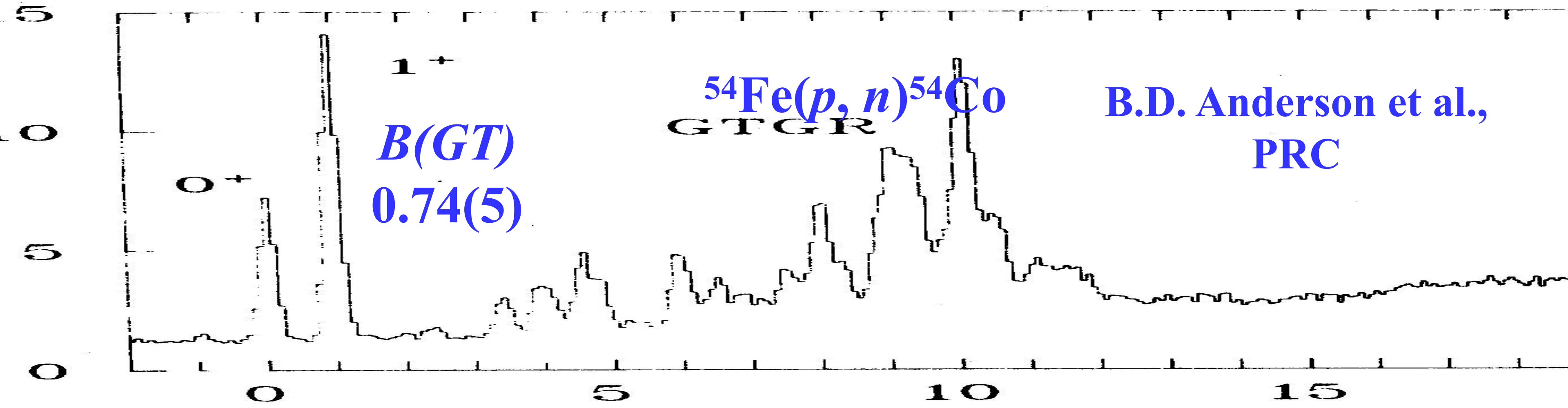

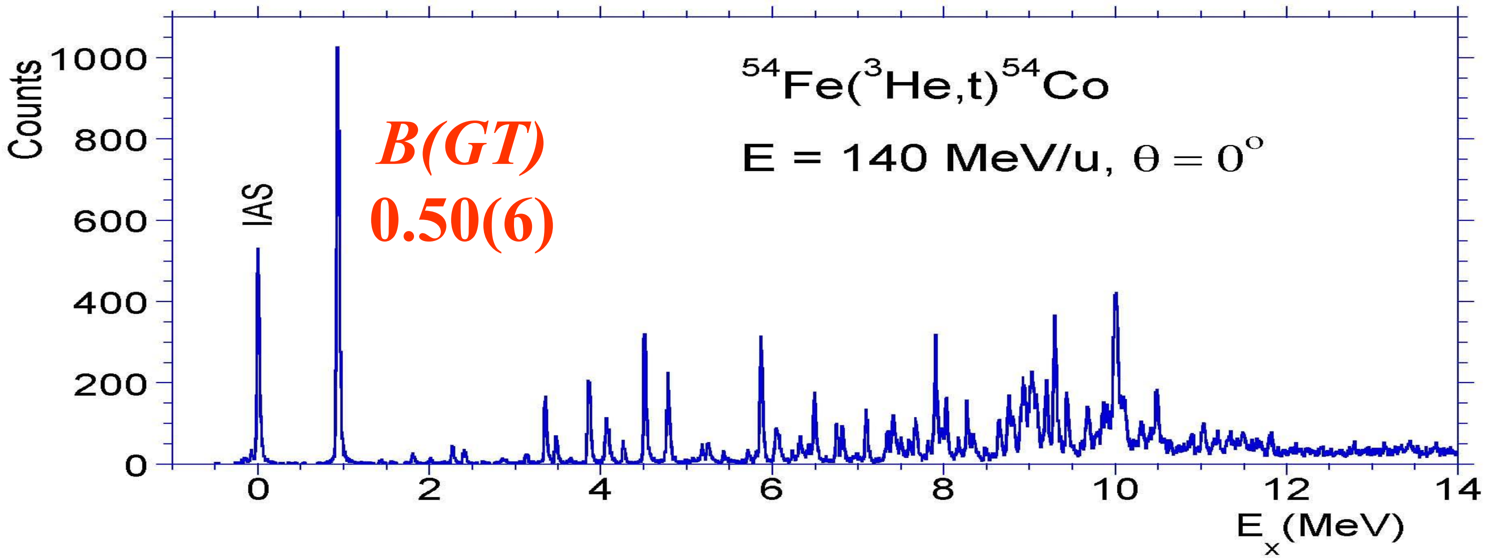

university of groningen

^{26}Mg(p,n)^{26}Al & ^{26}Mg(^{3}He,t)^{26}Al spectra

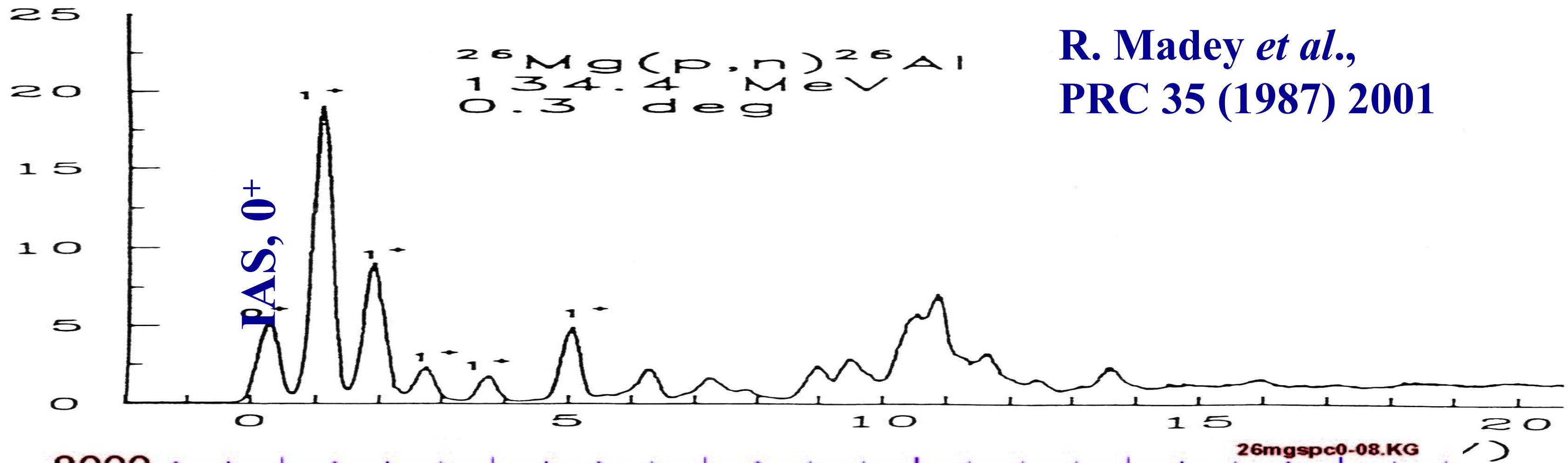

R. Madey *et al.*,
PRC 35 (1987) 2001

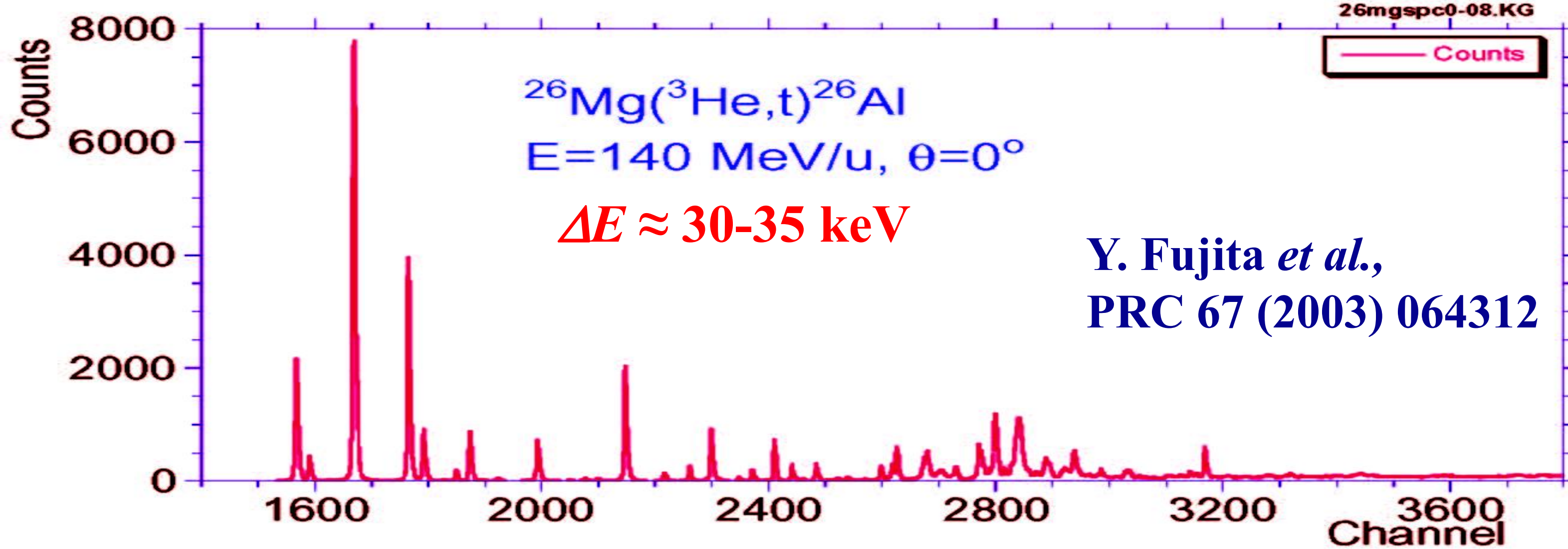

ΔE ≈ 30-35 keV

Y. Fujita *et al.*,
PRC 67 (2003) 064312

Prominent states are GT states and the IAS !

university of groningen

Experiments at RCNP, Osaka University

- (^{3}He,t) reaction at 420 MeV; measurements beyond 0°
  - High-resolution spectrometer “Grand Raiden”
  - $\Delta E \sim 30$ keV

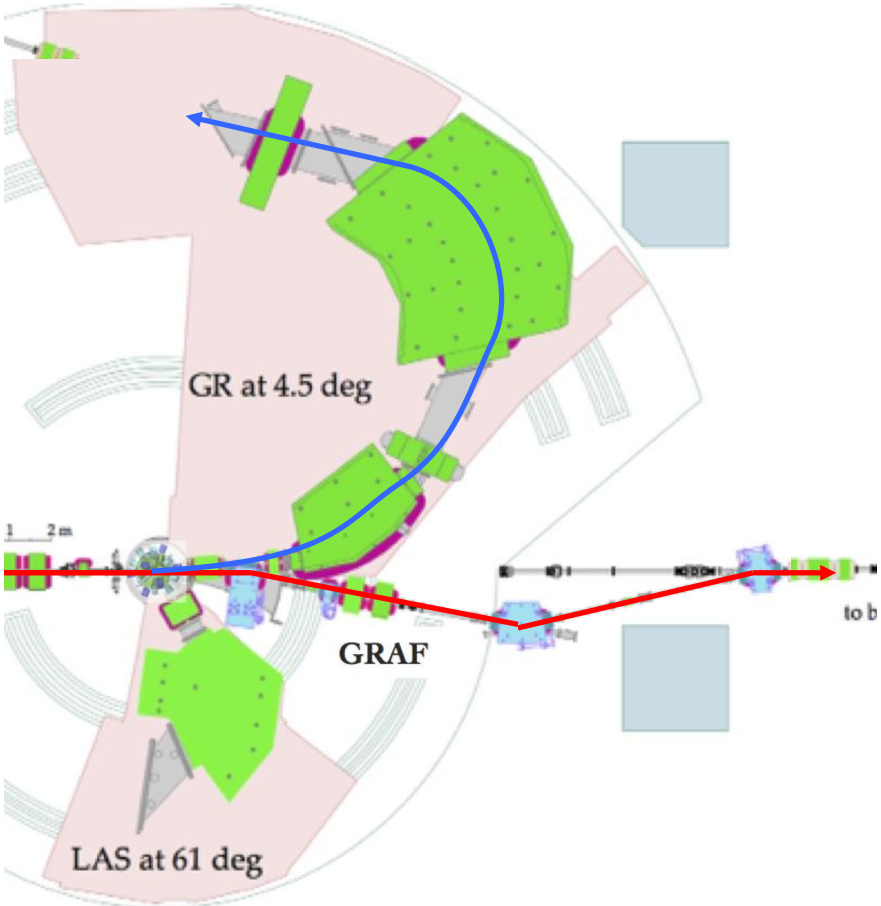

university of groningen

^{136}Xe(^{3}He,t)^{136}Cs

E(^{3}He) = 420 MeV

ΔE = 42 keV

$B_{exp}(GT+) =$

$$\frac{\mathrm{d}\sigma(q=0)}{d\Omega}\cdot\left[\frac{d\hat{\sigma}(GT)}{d\Omega}\right]^{-1}$$

extrapolated (DWBA)

unit cross section

ΔL = 2 & ΔL = 0 incoherent

P. Puppe *et al.*, Phys. Rev. C 84 (2011) 051305(R)

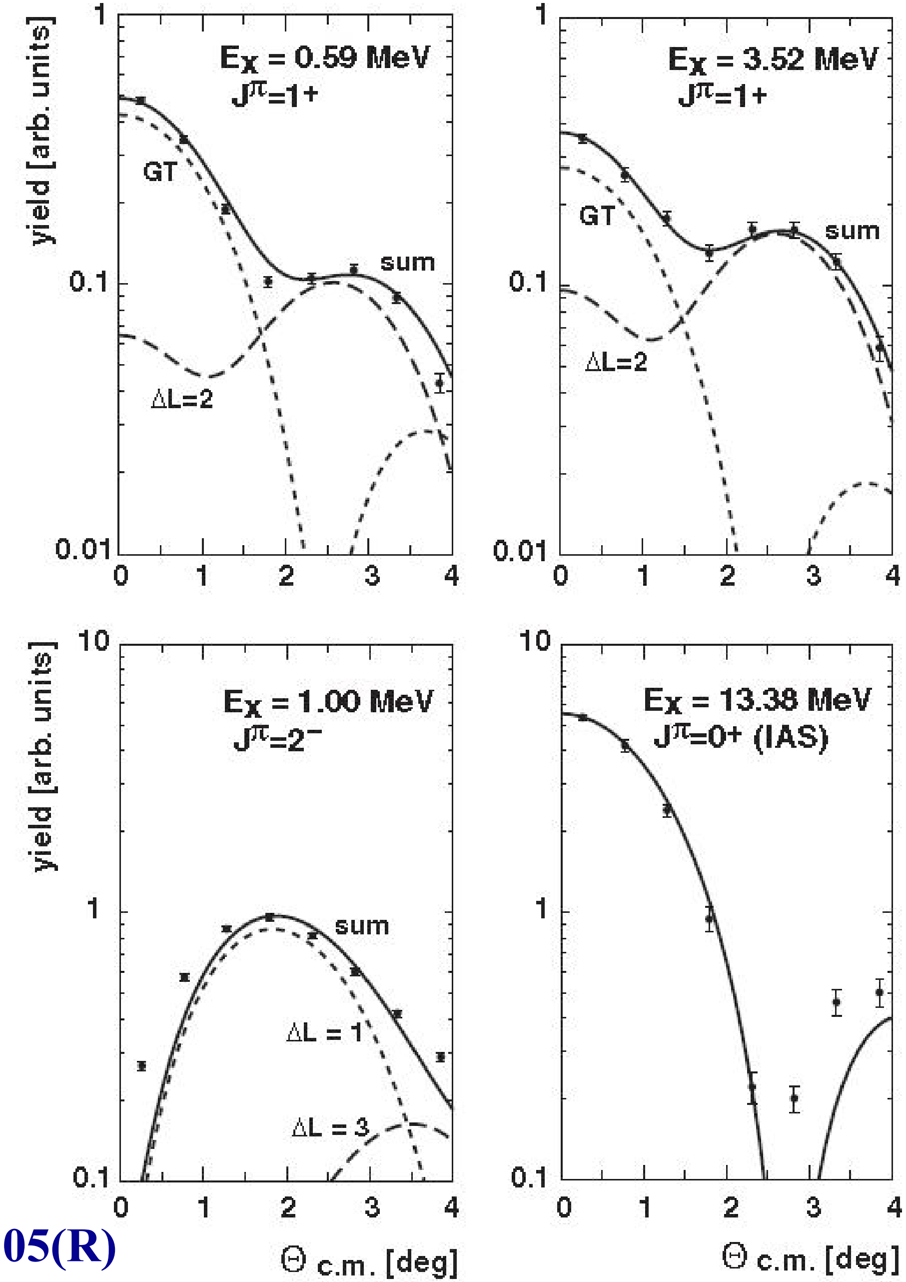

university of groningen

Double-beta decay nuclei ^{76}Ge, ^{82}Se, ^{100}Mo, ^{128}Te, ^{130}Te, ^{150}Nd show clear spin-dipole and Gamow-Teller states

- **RCNP high-resolution system is the unique and only opportunity to determine 2^- levels.**

^{128}Te

2^-

^{130}Te

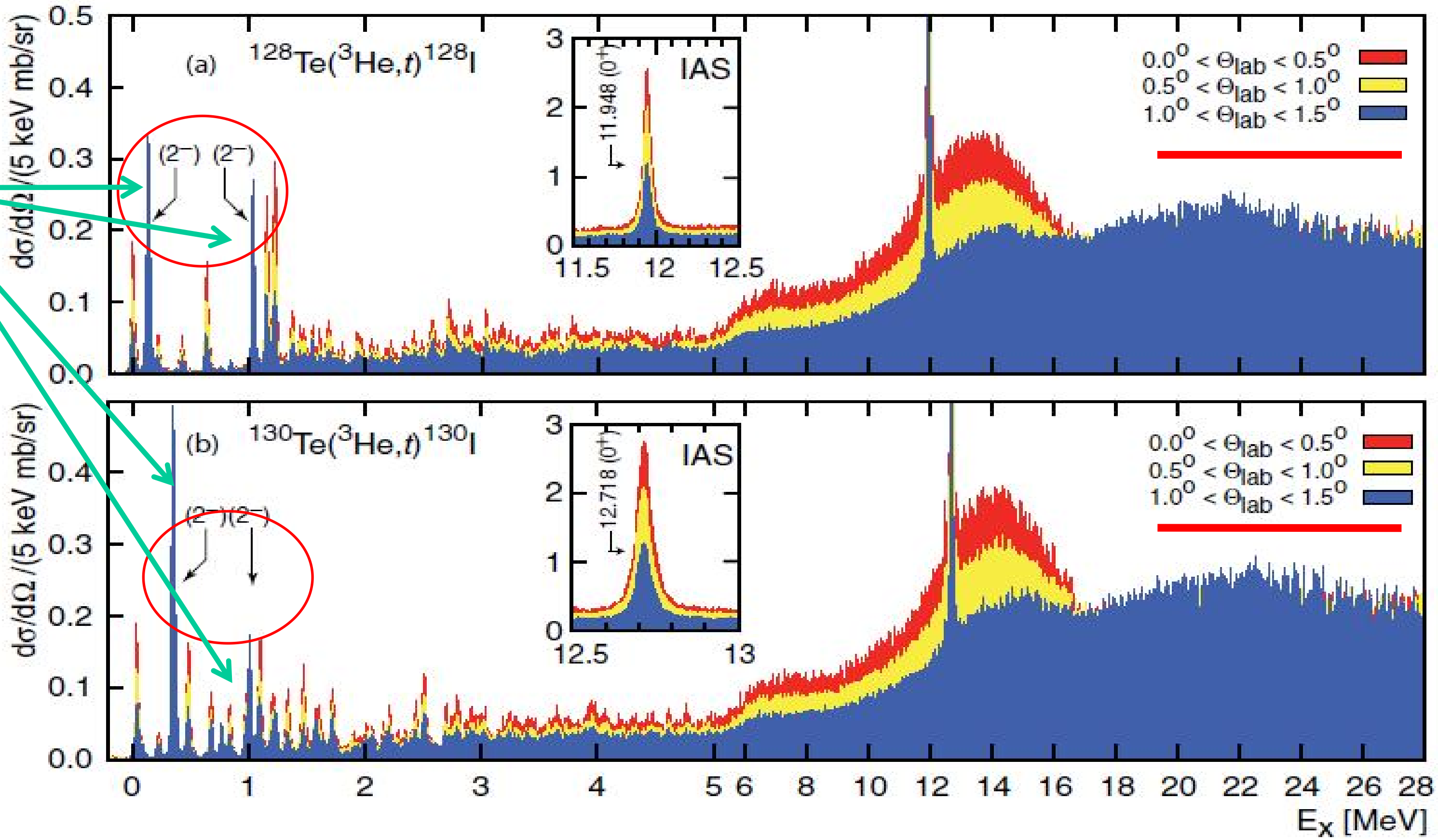

P. Puppe *et al.*, Phys. Rev. C 86 (2012) 044603

Measured angular distributions

- **Select spin-dipole (SD) component and derive B(SD) from DWBA fit at the peak region where SD $\langle \sigma\tau Y_1 \rangle^{2-}$ is dominant.**

  - **Angular distributions of SD are peaked around 2 deg.**
  - **Small deviation of (0.1 mb/sr) at 0.5 deg!**

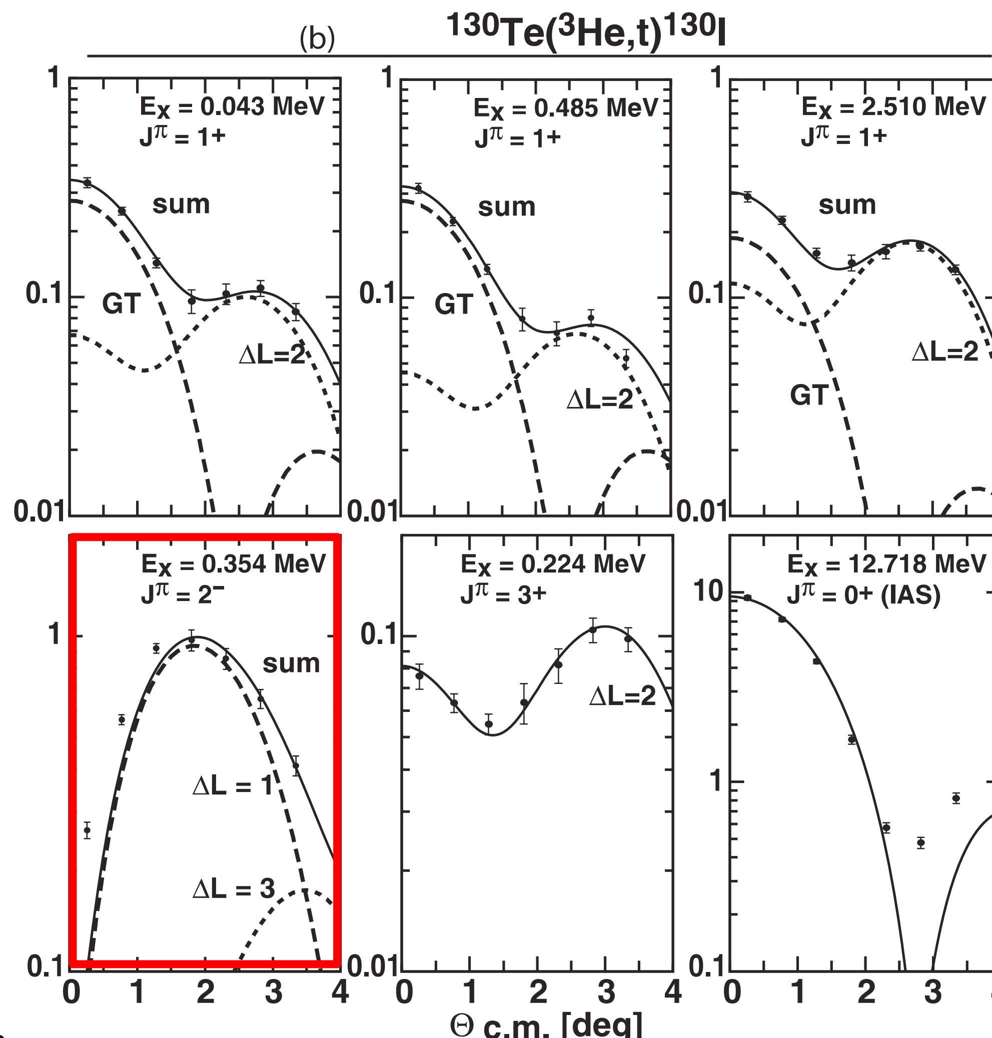

P. Puppe *et al*., Phys. Rev. C 86 (2012) 044603

Measured recently excitation-energy spectrum for the ^{116}Sn(^{3}He,t)^{116}Sb reaction for different ranges of the scattering angle θ at 140 MeV/u.

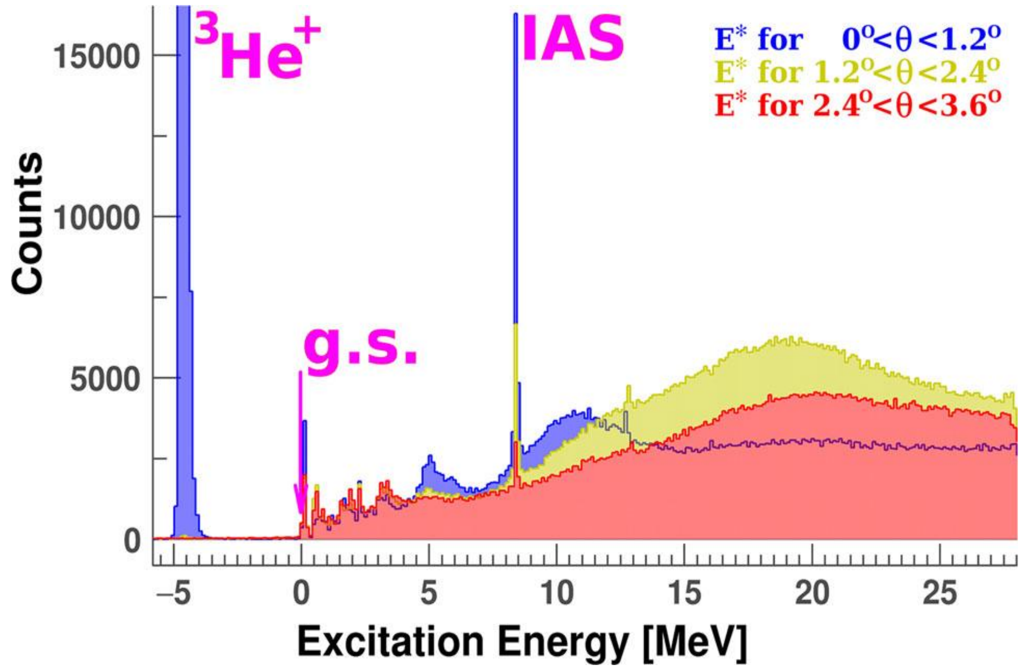

Same for ^{122}Sn(^{3}He,t)^{122}Sb at 140 MeV/u.

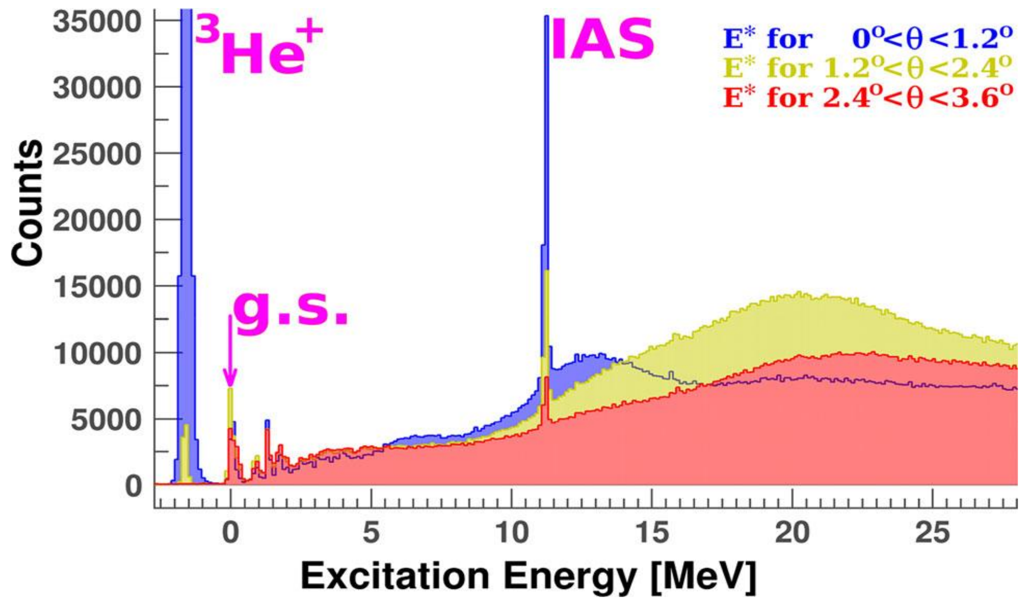

C.A. Douma, et al.,
Eur. Phys. J. A (2020) 56:51

Different multipolarity components used in MDA. The distributions were computed with FOLD code and smeared with the detector resolution ($\sigma = 0.2^\circ$ for the ^{116}Sn target and $\sigma = 0.3^\circ$ for the ^{122}Sn target). The angular distributions plotted on a linear scale correspond to the ^{116}Sn target at an excitation energy of zero MeV and have been plotted such that the peaks have equal heights.

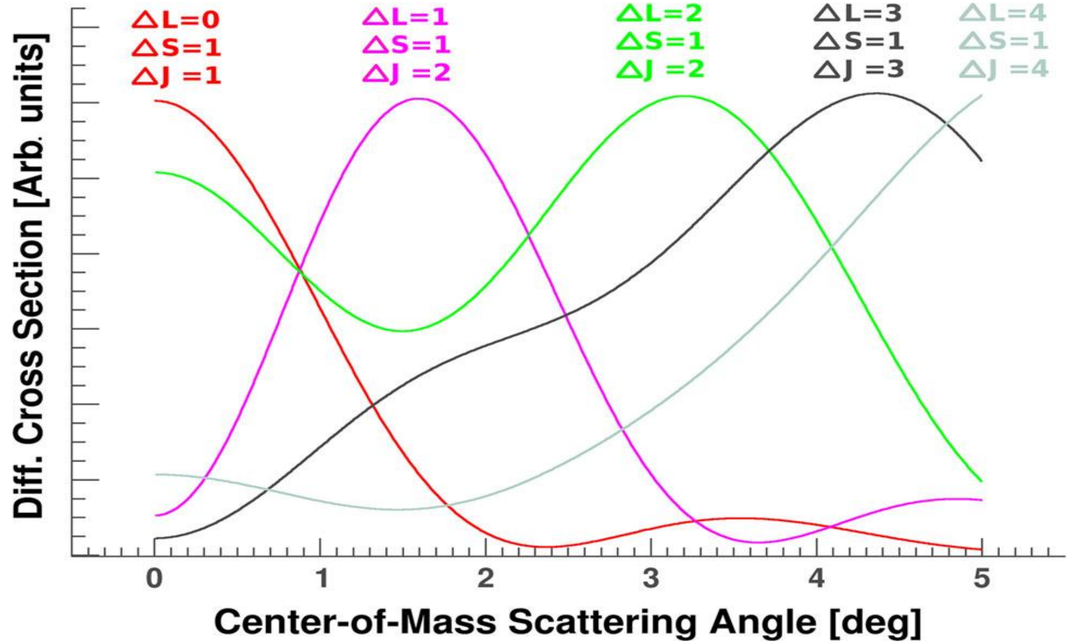

Angular distribution of the differential cross section of the level at 0.090 MeV and the performed MDA with $\Delta L = 0$ and $\Delta L = 2$ contributions.

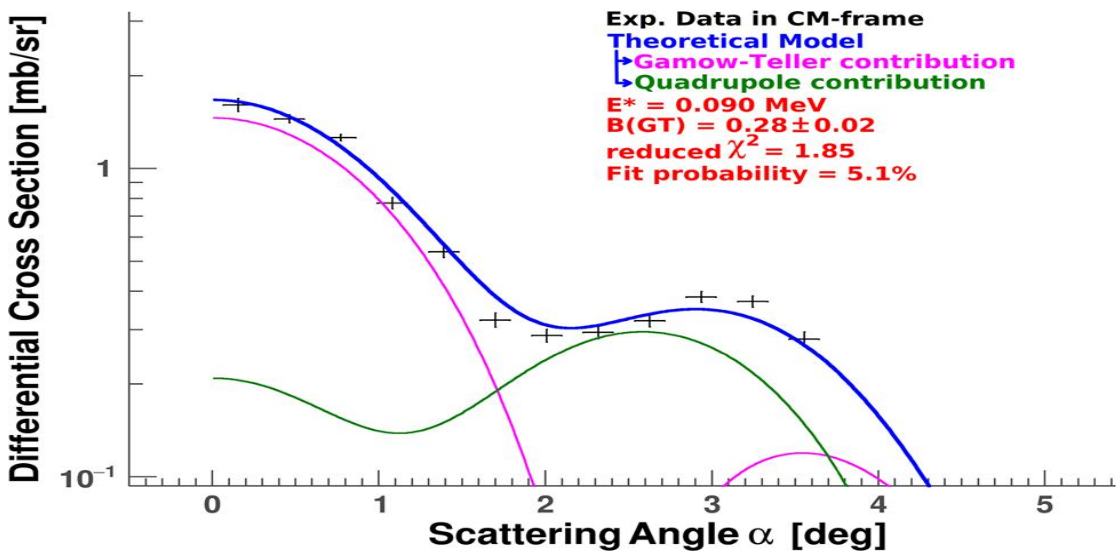

university of groningen

Extracted differential cross section of the IAS for the $^{116}Sn(^{3}He,t)^{116}Sb$ reaction at 140 MeV/u. The theoretical differential cross section is computed with Code FOLD, and fitted to the data with an overall normalisation as the only variable parameter. The fit probability is the area under the reduced χ^2 distribution.

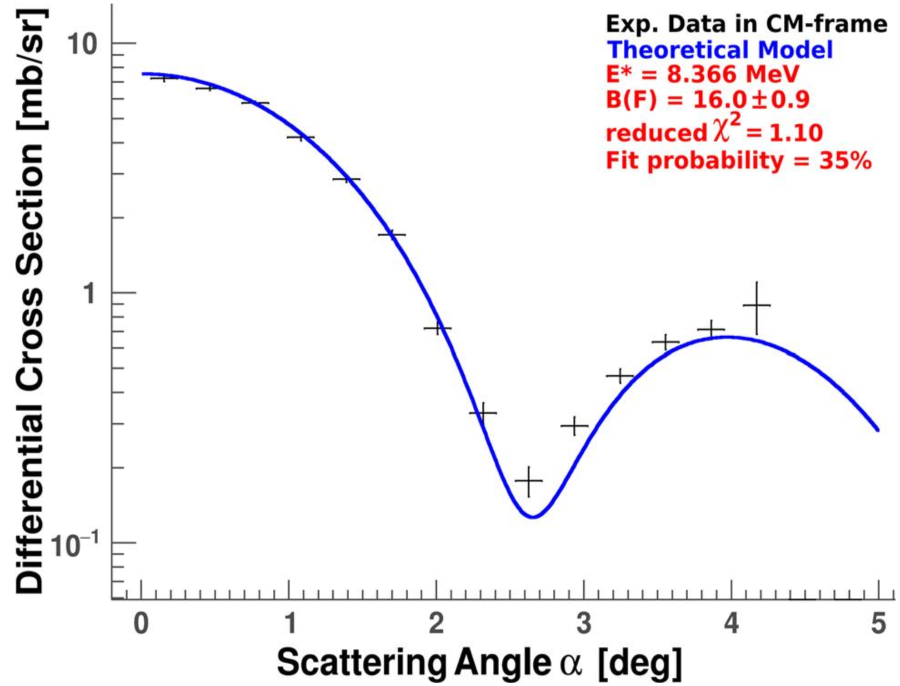

Same but for the $^{122}Sn(^{3}He,t)^{122}Sb$ reaction.

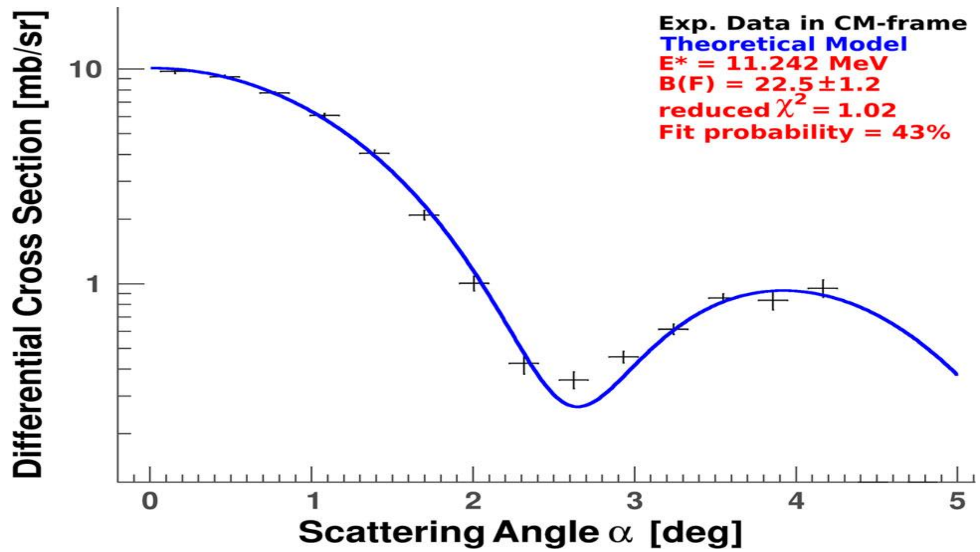

Fermi sum rule:

$$S_-(F) - S_+(F) = (N - Z)$$

For ^{116}Sn => 66 - 50 = 16 (16.0±0. 9)

For ^{122}Sn => 72 - 50 = 22 (22.5 ±1.2)

university of groningen

Different multipolarity contributions to the differential cross section for the $^{116}Sn(^{3}He,t)^{116}Sb$ reaction at 140 MeV/u determined with MDA without subtraction of the quasi-free background. The $\Delta L = 3$ and $\Delta L = 4$ contributions are very small.

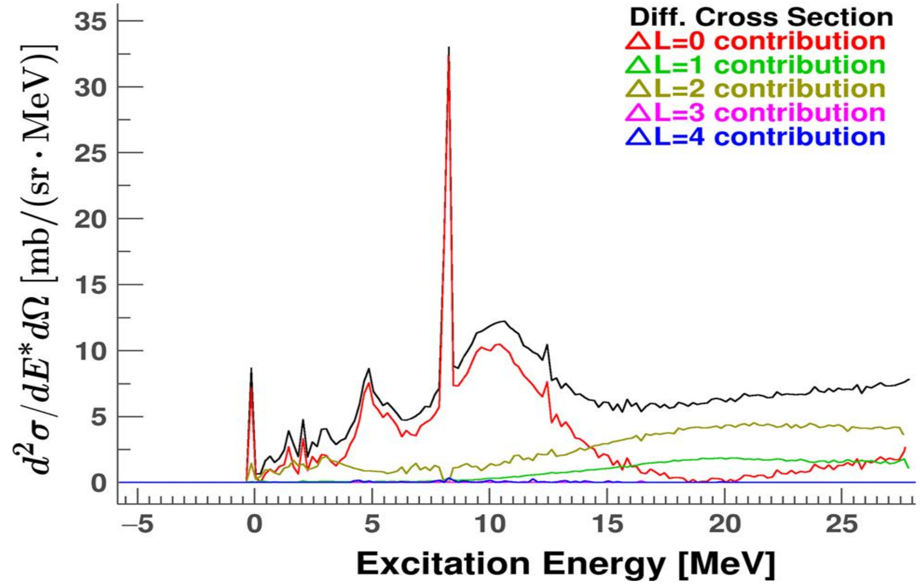

Same but for $^{122}Sn(^{3}He,t)^{122}Sb$ reaction at 140 MeV/u.

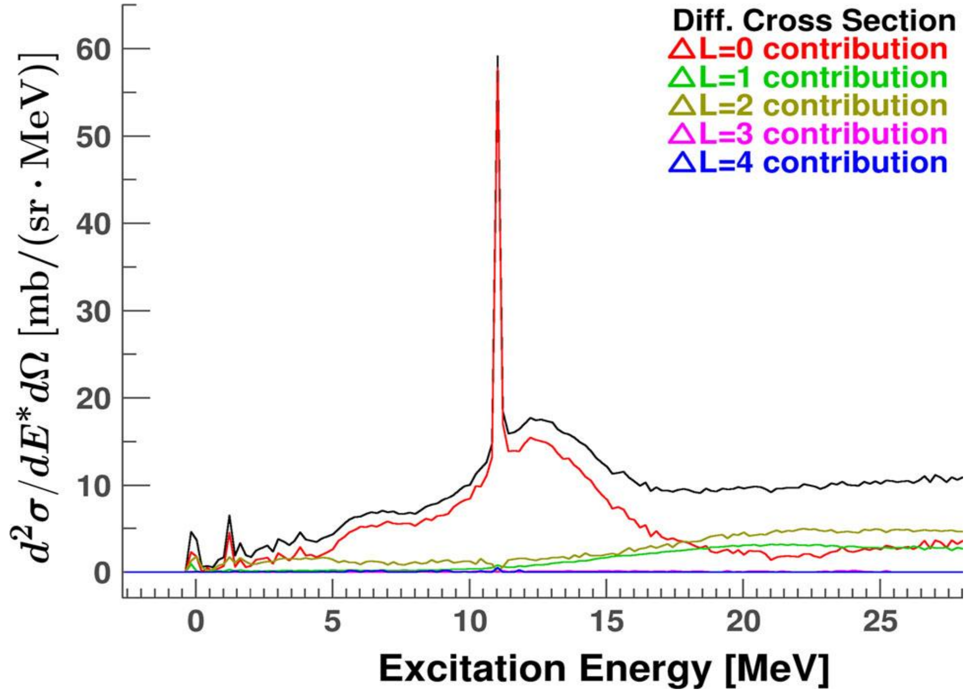

university of groningen

Comparison between experimental data (measured with (^{3}He,*t*) reaction at 140 MeV/u) and QRPA+QPVC calculations for the Gamow–Teller strength distribution of ^{116}Sb. **In order to compare with experimental data, the theoretical calculations were artificially normalised to $(0.75)^2 \cdot 3|N-Z|$** **The quasi-free background was not subtracted. The higher B(GT) 'ΔL = 0' strength could possibly be due to the low-energy tail of the IV(S)GMR ($2\hbar\omega$), which was not included in the calculations**

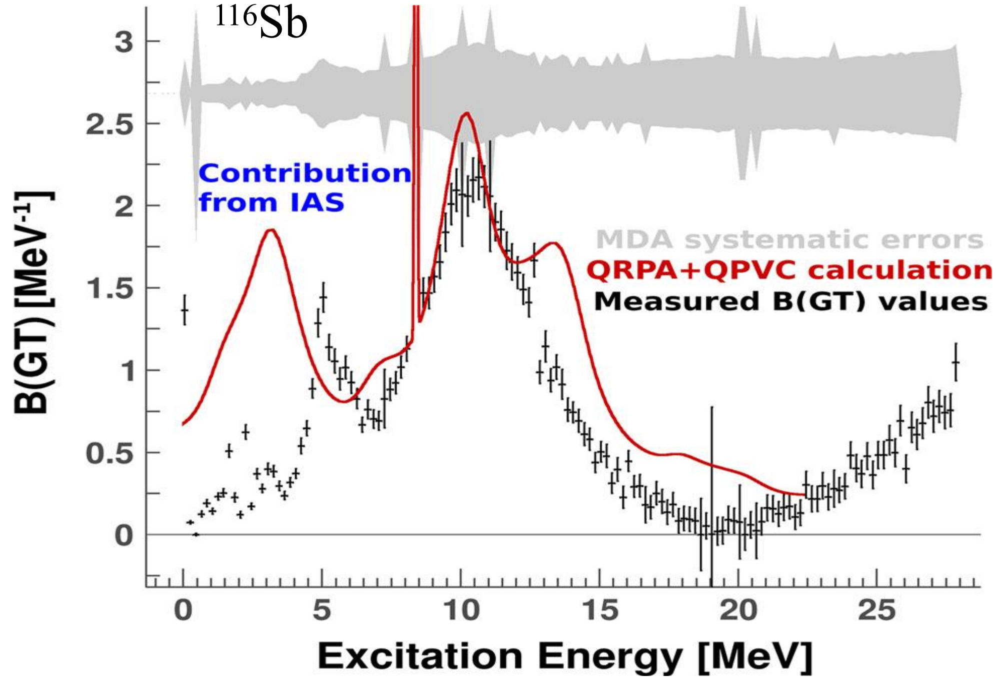

Same but ^{122}Sb.

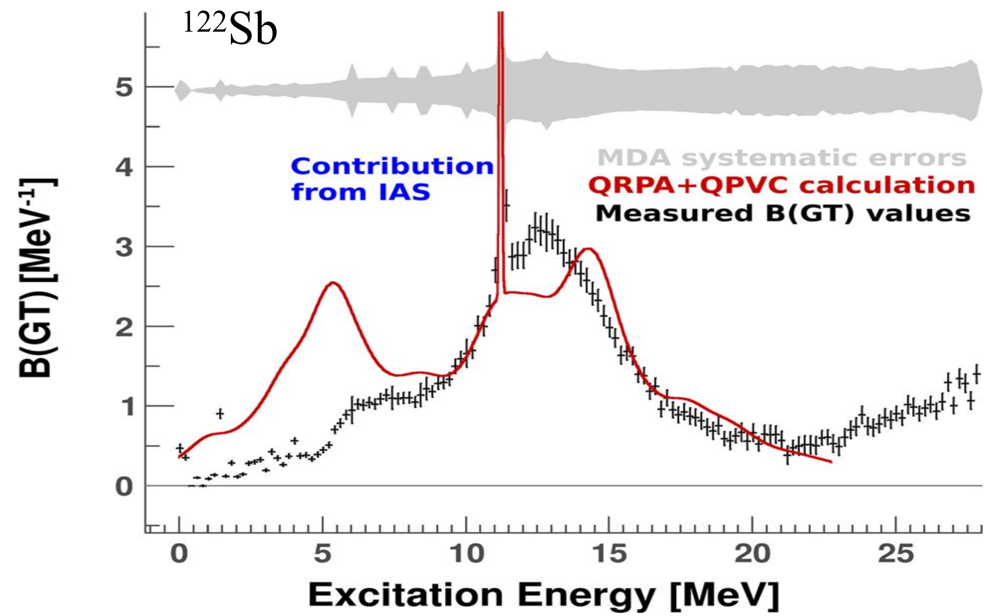

university of groningen

IV(S)GDR & GTR
Neutron-Skin Thickness

Determining neutron-skin thickness from IVSGDR

Summed ΔL=1 strength depends on the neutron-skin thickness as follows:

$$S^{-}_{IVSGDR} - S^{+}_{IVSGDR} = \frac{9}{2\pi}\left(N\langle r^2\rangle_n - Z\langle r^2\rangle_p\right)$$

Here, S^{-} and S^{+} are the spin-dipole total strengths in β^{-} and β^{+} channels.

Using the calculated B = S^{+}/S^{-} ratios the neutron-skin thicknesses can be deduced from the above equation:

$$\langle r^2\rangle_n^{1/2} - \langle r^2\rangle_p^{1/2} = \frac{\alpha\sigma_{exp}(1-B) - (N-Z)\langle r^2\rangle_p}{2N\langle r^2\rangle_p^{1/2}}$$

university of groningen

IVSGDR method => $^{A}Sn(^{3}He,t)$

Performed at RCNP
At 450 MeV

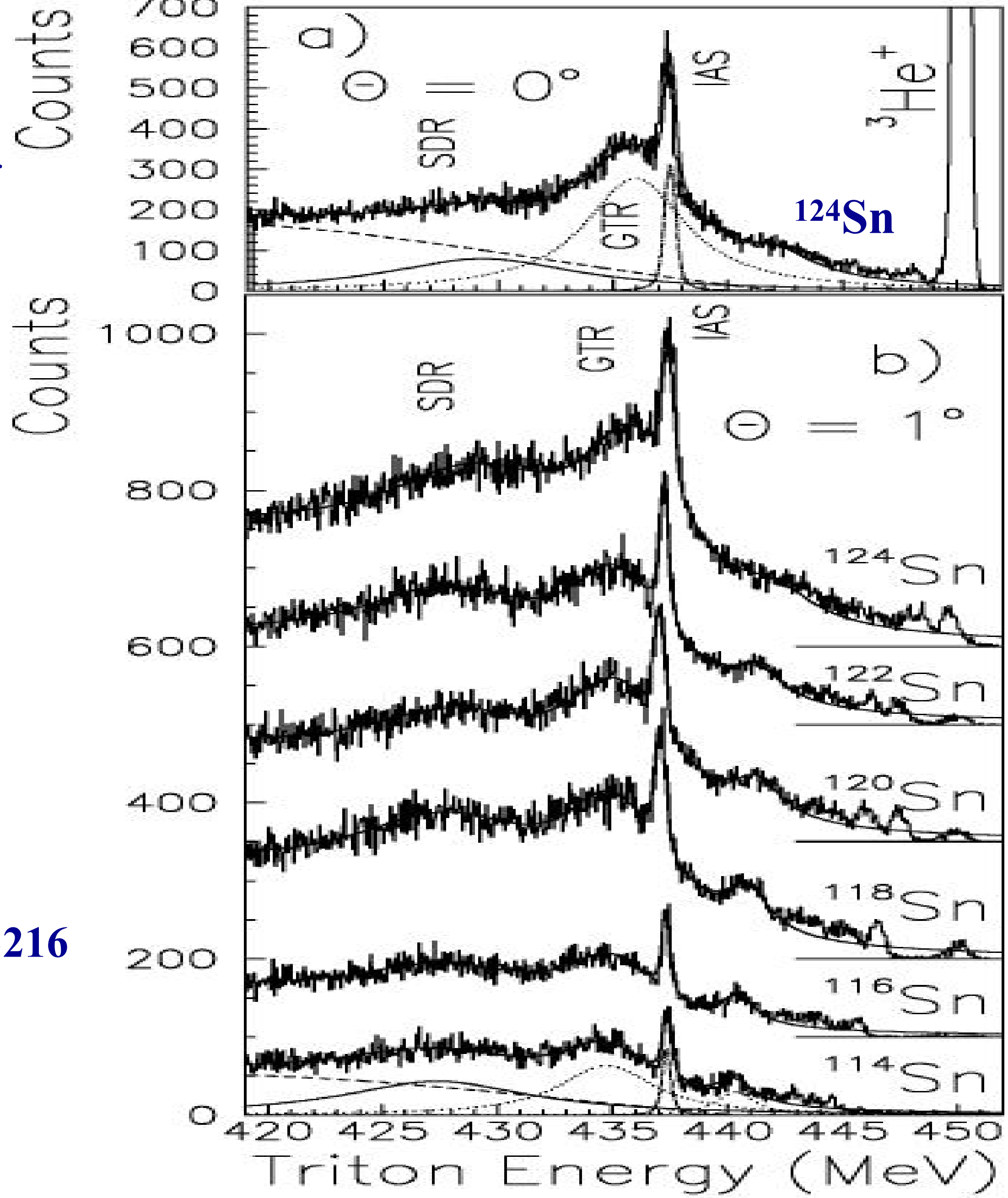

A. Krasznahorkay et al.,
Phys. Rev. Lett. 82 (1999) 3216

university of groningen

Summary of the neutron-skin thicknesses ($\langle r_n^2\rangle^{1/2} - \langle r_p^2\rangle^{1/2}$ in fm) obtained in different methods.

Isotope	(p,p) [4,5]	(p,p) [7]	GDR [16]	SDR [18]	antiproton [11]
^{112}Sn					0.09±0.02
^{114}Sn				≤0.09	
^{116}Sn	0.15±0.05		0.02±0.12	0.12±0.06	0.12±0.02
^{118}Sn				0.13±0.06	
^{120}Sn				0.18^{a})	0.12±0.02
^{122}Sn				0.22±0.07	
^{124}Sn	0.25±0.05		0.21±0.11	0.19±0.07	0.19±0.02
^{208}Pb	0.14±0.04	0.20±0.04	0.19±0.09		0.15±0.02

^{a}) Normalized to the theoretical value of Angeli et al. [21].

4. L. Ray et al., Phys. Rev. C 19 (1979) 1855.
5. G.W. Hoffmann et al., Phys. Rev. Lett. 47 (1981) 1436.
7. V.E. Stradubski and N.M. Hintz, Phys. Rev. C 49 (1994) 2118.
11. A. Trzcinska et al., Phys. Rev. Lett. 87 (2001) 82501.
16. A. Krasznahorkay et al., Nucl. Phys. A 567 (1994) 521. GDR => IVGDR
18. A. Krasznahorkay et al., Phys. Rev. Lett. 82 (1999) 3216. SDR => IVSGDR

The full dots with error bars show the neutron-skin thicknesses of the Sn isotopes determined from the IVSGDR data, obtained in a ^{A}Sn(^{3}He,*t*) experiment performed at KVI at 177 MeV, as a function of the mass number.

The experimental values determined by the (*p*,*p*), and the antiprotonic methods are shown as full triangles and full squares with error bars, respectively. The numbered full lines represent different theoretical results.

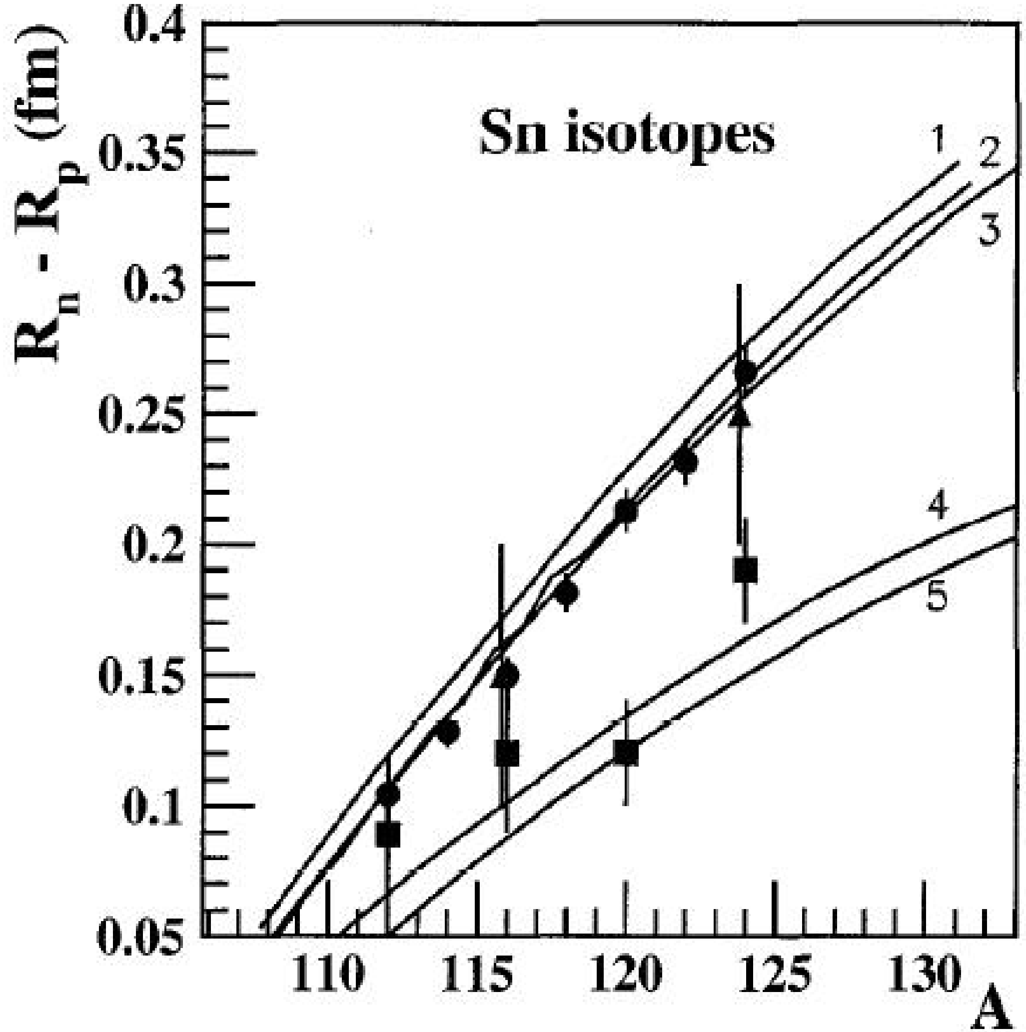

A. Krasznahorkay *et al.*, Nucl. Phys. A731 (2004) 224

university of groningen

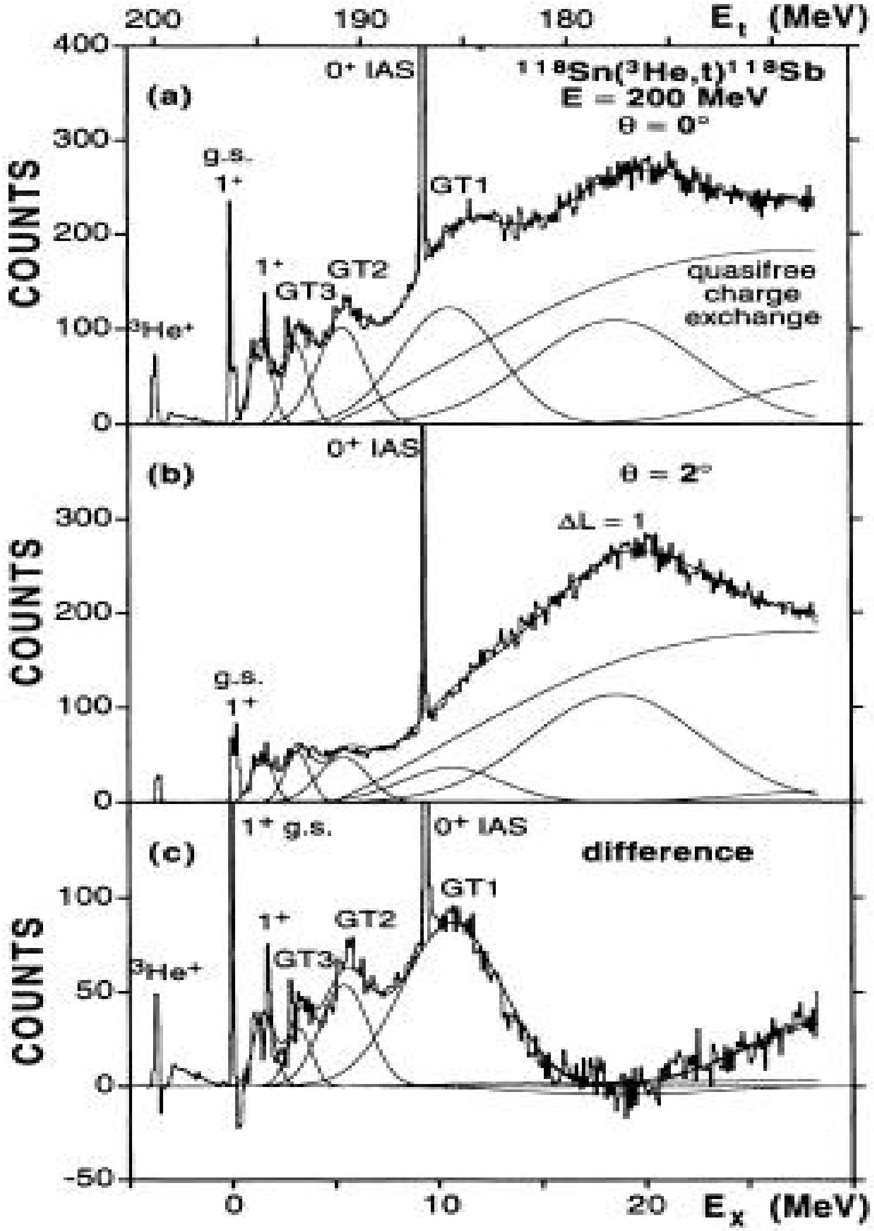

K. Pham *et al*., PRC 51 (1995) 526

(^{3}He,*t*) charge-exchange reaction on all stable Sn nuclei at IUCF, Bloomington

E(^{3}He) = 200 MeV

Excitation-energy spectra are plotted relative to IAS.

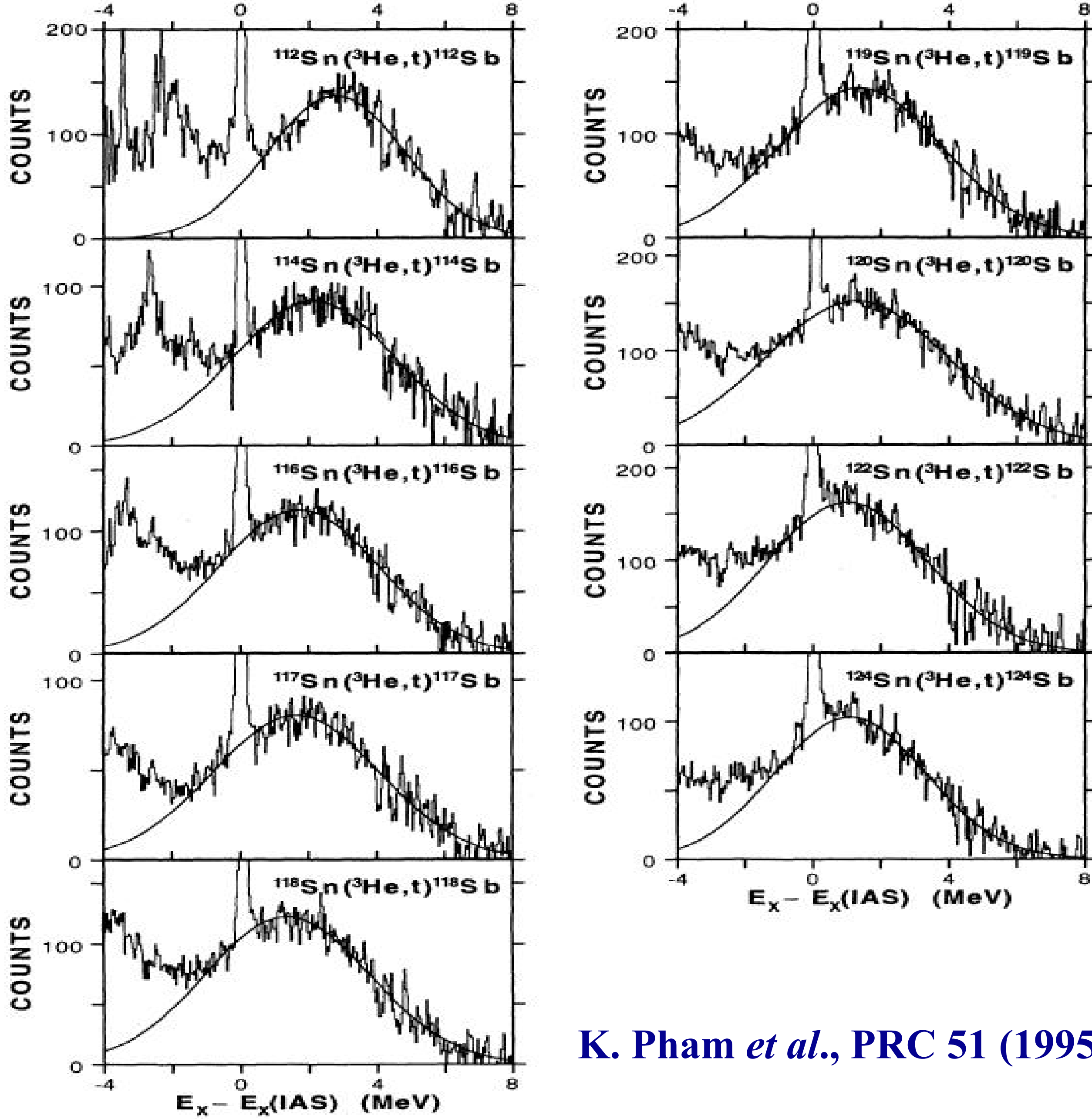

K. Pham *et al.*, PRC 51 (1995) 526

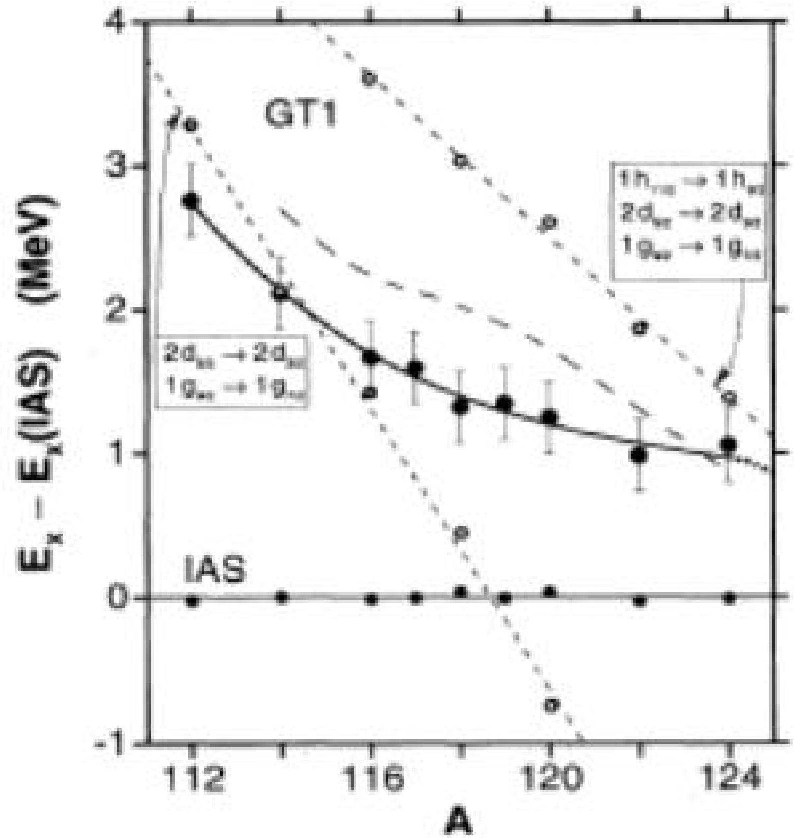

Excitation energy of main component of GTR relative to IAS.

K. Pham *et al*., Phys. Rev. C51 (1995) 526

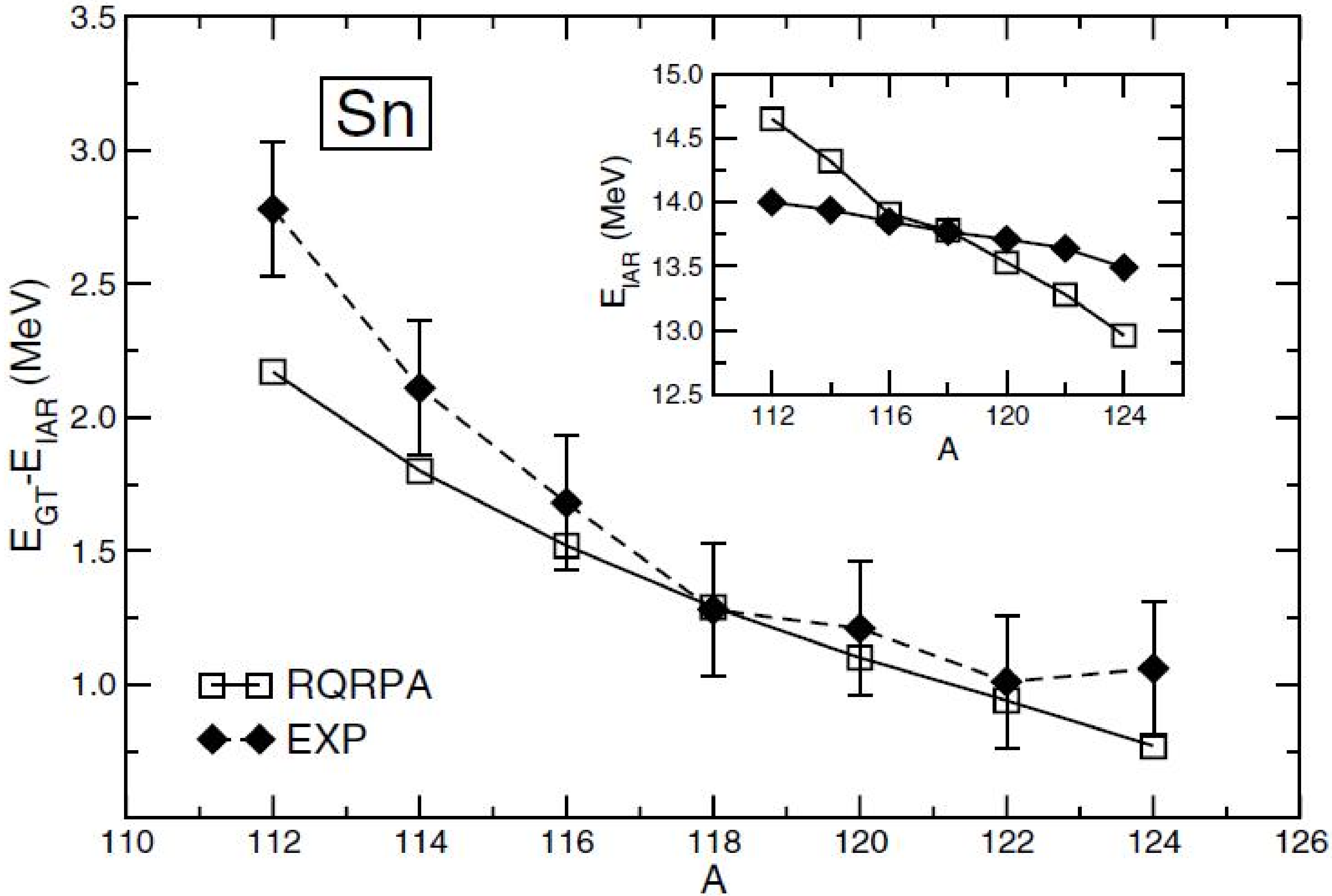

Comparison of theoretical calculations to experimental results for excitation energy of main component of GTGR relative to IAS. Inset shows IAS energies

D. Vretenar *et al*., Phys. Rev. Lett. 91 (2003) 262502

Theoretical pn-RQRPA and experimental differences of GTR and IAS excitation energies as function of neutron-skin thickness (data from K. Pham). Lower panel shows comparison between theoretical neutron-skin thickness and experimental data.
(data from A. Krasznahorkay)

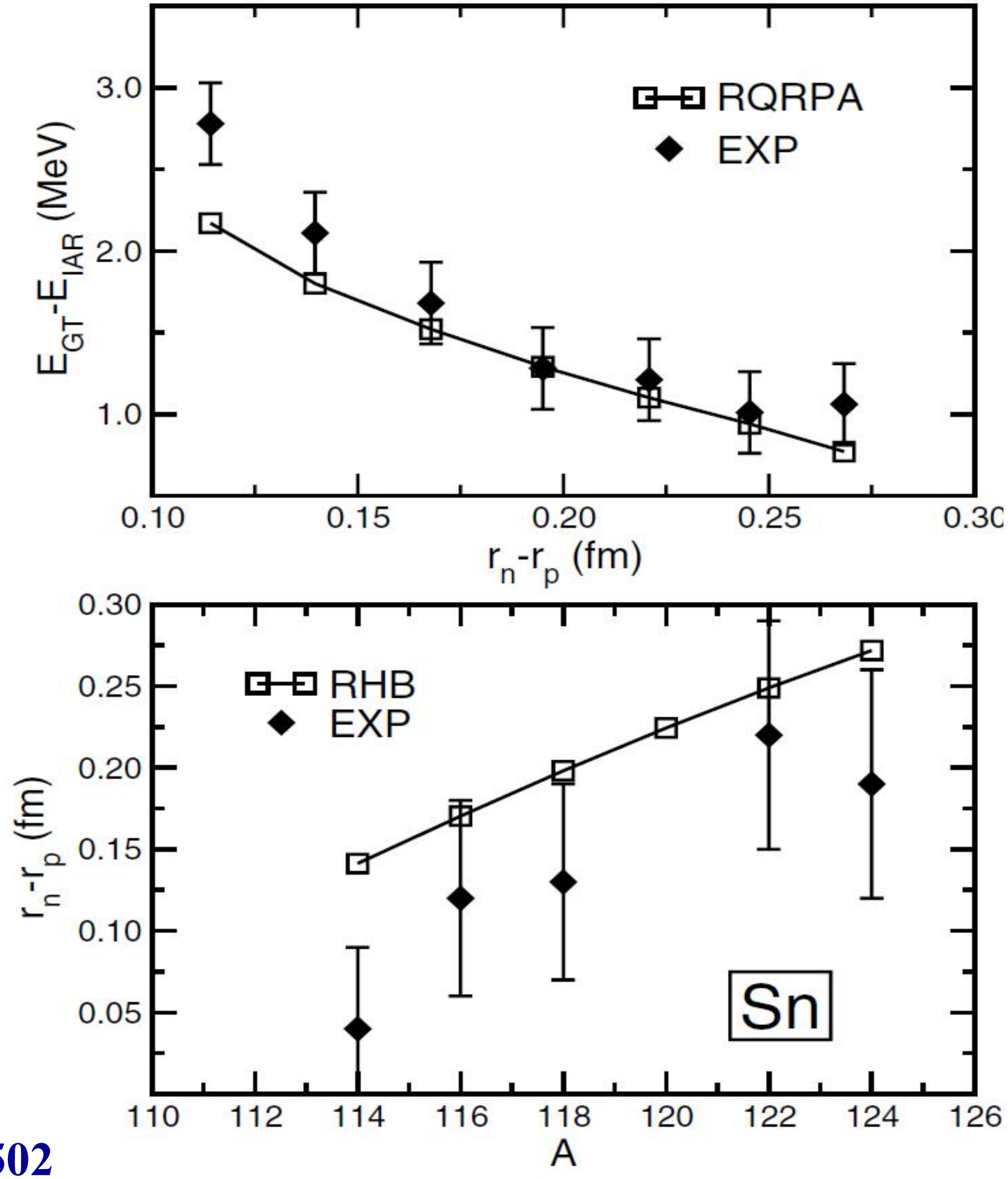

D. Vretenar *et al.*, PRL 91 (2003) 262502

A. Krasznahorkay *et al.*, PRL 83 (1999) 3216; r_n-r_p

Outlook

Radioactive ion beams will be available at energies where it will be possible to study GT transitions (RIKEN, FRIB, FAIR, EURISOL)

- **Determine GT strength in unstable *sd* & *fp* shell nuclei**
- **Use IV(S)GDR as tool to determine *n*-skin [IV(S)GDR]**

Thank you for your attention

Intermezzo: Sum rules

Fermi, Gamow-Teller and higher multipole non-energy-weighted sum rules (NEWSR):

Gamow-Teller operator

$$\beta_{\pm}(\mu) = \frac{1}{2}\sum_{k=1}^{A} \sigma_{\mu k}\tau_{\pm k}$$

$$(\mu =- 1,0, + 1), \;\; \tau_{\pm} = (\tau_x \pm i\tau_y)$$

$$\frac{1}{2}\tau_{-}|n\rangle = |p\rangle, \;\; \frac{1}{2}\tau_{+}|p\rangle = |n\rangle, \;\; \tau_{-}|p\rangle = \tau_{+}|n\rangle = 0$$

$$S_{\pm}(GT) = \sum_{f,\mu} |\langle f|\beta_{\pm}(\mu)|i\rangle|^{2}$$

$$S_{\pm}(GT) = \sum_{f,\mu} \langle f|\beta_{\pm}(\mu)|i\rangle^{*} \langle f|\beta_{\pm}(\mu)|i\rangle$$

$$S_{\pm}(GT) = \sum_{f,\mu} \langle i|\beta_{\pm}^{\dagger}(\mu)|f\rangle \langle f|\beta_{\pm}(\mu)|i\rangle$$

Using closure:

$$S_{\pm}(GT) = \sum_{\mu} \langle i | \beta_{\pm}^{\dagger}(\mu) \beta_{\pm}(\mu) | i \rangle$$

$$\tau_{\mp}^{\dagger} = \tau_{\pm}$$

$$S_{-}(GT) - S_{+}(GT) = \sum_{\mu} \langle i | \beta_{-}^{\dagger}(\mu) \beta_{-}(\mu) - \beta_{+}^{\dagger}(\mu) \beta_{+}(\mu) | i \rangle$$

$$S_{-}(GT) - S_{+}(GT) = \frac{1}{4} \left\langle i \middle| \sum_{k=1}^{A} \sum_{\mu=-1}^{+1} \left[\sigma_{\mu k}^{\dagger} \tau_{+k} \sigma_{\mu k} \tau_{-k} - \sigma_{\mu k}^{\dagger} \tau_{-k} \sigma_{\mu k} \tau_{+k} \right] \middle| i \right\rangle$$

$$S_{-}(GT) - S_{+}(GT) = \frac{1}{4} \langle i | \sum_{k=1}^{A} \left[\sigma_{k}^{2} \tau_{+k} \tau_{-k} - \sigma_{k}^{2} \tau_{-k} \tau_{+k} \right] | i \rangle$$

$$S_{-}(GT) - S_{+}(GT) = \frac{3}{4} \langle i | \sum_{k=1}^{A} \left[\tau_{+k} \tau_{-k} - \tau_{-k} \tau_{+k} \right] | i \rangle$$

$$\sigma^2 = \sum_{\mu=-1}^{+1} [\sigma_\mu^\dagger \sigma_\mu]\,; \quad \textit{expectation value of } \sigma^2 \textit{ is } 3.$$

$$\tau_+\tau_-|n\rangle = 4|n\rangle,\ \ \tau_-\tau_+|p\rangle = 4|p\rangle,\ \ \tau_+\tau_-|p\rangle = \tau_-\tau_+|n\rangle = 0$$

$$S_-(GT) - S_+(GT) = \frac{3}{4} \times 4\,(N - Z) = 3(N - Z)$$

This is the Ikeda sum rule. For the Fermi sum rule:

$$S_\pm(F) = \frac{1}{4} \sum_{f,\mu} |\langle f|\tau_\pm|i\rangle|^2$$

$$S_-(F) - S_+(F) = \frac{1}{4} \times 4\,(N - Z) = (N - Z)$$

Isovector non-spin-flip and isovector spin-flip higher multipole operators:

$$O_{\pm}^{\lambda t}(M) = \frac{1}{2}\sum_{k=1}^{A} r_k^{\lambda} Y_{\lambda M}(\hat{r}_k)\tau_{\pm k}$$

$$O_{\pm}^{\lambda\sigma t}(M\mu) = \frac{1}{2}\sum_{k=1}^{A} r_k^{\lambda}[Y_{\lambda}(\hat{r}_k)\otimes\vec{\sigma}_k]_{J^{\pi}}\tau_{\pm k}$$

$$S_{-}^{\lambda J} - S_{+}^{\lambda J}(J) = \frac{3(2J+1)}{2\pi}\left(N\langle r_n^{2\lambda}\rangle - Z\langle r_p^{2\lambda}\rangle\right)$$

If spin-flip is involved the sum over possible *J*-values yields a factor 3(2λ+1).